



Nucleosynthesis involving mainly neutron capture processes III

Ramen Kumar Parui

Centre for Research in Astrophysics and Philosophy, ACS, Imphal Airport,
Tulihal, Imphal-795 140, India

Received 16 October 1996, accepted 11 March 1997

Abstract : In preceding papers (Paper I [1] and Paper II [2]) we have reviewed the important role of neutron capture nucleosynthesis in different evolving stages of stellar evolution (*i.e.* main sequence stage, red giant phase, supernova stage and neutron star phase) and production of heavy elements. In particular, we have explored how neutrons produced in one stage come into next stage as remnant and play an active role to begin nucleosynthesis in the next stage for ultimate neutron star formation as well as various difficulties and uncertainties in different evolving phases. A lot of improvements in nucleosynthetic physics have been occurred during the last year with the help of advanced techniques and numerical simulations. In the present paper, we have attempted to present a progress report on it and the remaining difficulties and uncertainties which are to be solved for understanding the stellar nucleosynthetic physics.

Keywords : Nucleosynthesis, supernova remnants, neutron star

PACS Nos. : 95.30.Cq, 97.60.Jd, 98.38.Mz

Plan of the Article

1. **Introduction**
2. **Recent Abundances**
 - 2.1. *Recent r-process abundances*
3. **An over view of earlier problems**
 - 3.1. *Star formation*
 - 3.2. *Pre-hydrogen and hydrogen burning phase*
 - 3.3. *Helium core burning phase*
 - 3.3.1. *Production of ^{12}C , ^{16}O , ^{20}Ne , etc*
 - 3.3.2. *Production of ^{13}C*
 - 3.3.2.1. *Hot C-N-O cycle and non-standard mixing*

3.3.3. *Production of ^{21}Ne , ^{22}Ne as alternative*

3.4. *Carbon and oxygen burning*

3.5. *Influence of new rates*

3.5.1. *He core burning :*

$^{13}\text{C}(\alpha, n) ^{16}\text{O}$, $^{22}\text{Ne}(\alpha, n) ^{25}\text{Mg}$ and other reactions

3.5.2. *Carbon and Ne shell burning*

3.5.3. *Oxygen shell burning*

4. **Recent progress**

4.1. *Star formation*

4.2. *Abundances*

4.3. *Helium burning*

4.4. *Carbon burning*

4.5. *Oxygen burning*

4.6. *Supernova phase*

4.7. *Proto-neutron star phase*

5. **Conclusion and outlooks**

1. **Introduction**

Nucleosynthesis plays an important role in order to understand the physics of stellar evolution, nuclear element synthesis as well as generation of heavy elements during stellar evolution and the origin of elements in stars. It is believed from the abundance curve of the nuclei found in nature that most of the nuclei are the product of a sequence of more or less discrete processes occurring inside the stars. Three distinct contributors for the production of heavy elements involving neutron addition to the seed elements previously ^{56}Fe are the s-process (slow neutron capture process [3,4]), the r-process (the rapid neutron capture process [4]), and the p-process (for the production of proton-rich heavy isotopes *i.e.* the p-nuclei [5–7]). However, the major contributors are the s-process and r-process. It is also thought that in the stellar interior, most of the naturally occurring heavy elements other than Fe group nuclei, are synthesized through the slow (s-) and/or rapid (r-) neutron capture processes.

Although the s-process is one of the major nucleosynthetic processes, an environment with a much lower neutron density than the r-process is required for its occurrence. It is also occurred over a much longer time period. The recent abundance curve (Figure 1) analysis shows that the s-process is not a freeze out from the equilibrium *i.e.* the environment favours this slow neutron capture process to reach equilibrium but fails to achieve it. The main reason is the production of s-nuclei by the pre-existing seed nuclei through the capture of liberated neutrons during the reaction.

The fitting of σN curve to the solar system s-process abundance suggest different sites for the strong s-process component (or main component), weak s-process component

as well as necessity of neutron exposure. The main component (*i.e.* neutron exposure with $\tau_0 \approx 0.30 \text{ mb}^{-1}$) produces most of the nuclei in the mass range $90 < A < 204$ while the weak component (*i.e.* neutron exposure with $\tau_0 \approx 0.60 \text{ mb}^{-1}$) produces nuclei for $A \leq 90$. But recent result [8] indicates uncertainties in the weak s-process component reaction and shows that

- (i) the s-process is somewhat more robust than previously thought,
- (ii) the separation of the $A \leq 90$ s-nuclei into those coming from the weak and the main components, is more complicated.

The occurrence of the r-process depends on whether it is a primary or secondary process. The time scale associated with the r-process indicates to violent events for example supernova, winds from nascent neutron star, *etc.* These indicate that r-process is a primary process, freeze out from equilibrium process. If the system is quite neutron-rich, this r-process still occurs. In that case, the degree of neutron richness necessary for a r-process in a high entropy environment is less than in a low entropy system *i.e.* the degree of neutron richness for a primary r-process depends directly on the entropy per baryon [9]. For a low entropy environment the r-process needs Y_e as low as 0.1–0.2 [10,11] at the mass cut (*i.e.* the boundary between the matter that escapes into space from the supernova and the matter that remains as part of the remnant neutron star). But current picture is that the yield of Y_e from type II supernova is more than that expected above.

In this mass-cut difficulty, Woosley and Hoffman [12] suggested that winds from the nascent neutron stars arose due to r-process. So, a full survey of stellar nucleosynthesis is required in order to understand the above.

In this review, we have discussed only neutron capture nucleosynthesis through s-, p- and r- processes during stellar evolution *i.e.* from the birth of a star to neutron star stage. In Section 2 we have pointed out the new probable sites for s-, p- and r-processes alongwith latest available r-process abundances. In Section 3, we give an overview of the earlier problems in different evolving phase of stellar evolution while in Section 4, the discussion of recent developments have been achieved and new results we have obtained are mentioned. On the basis of new results, we have pointed out in the conclusion and future outlooks section, the remaining problems to be solved for understanding neutron capture nucleosynthesis.

2. Recent abundances

The observed atomic abundance pattern in nature, plays a crucial role to determine the success of nucleosynthesis. A sequence of burning processes, during the successive stages of stellar evolution, converts H to He, He to C, and so on, until the isotopes around iron are reached. These isotopes exhibit the highest binding energy per nucleon *i.e.* the most stable nuclei in nature. As a result, a large abundance occurs around $A = 56$. It is believed that these heavier nuclei can only be produced by successive neutron capture reactions and beta decay.

Figure 1 shows the modern abundance curve, schematically decomposed into s-process, p-process and r-process contributions [7], as a function of atomic mass. The population of s-nuclei, produced in a slow neutron capture process, exhibits an abundance

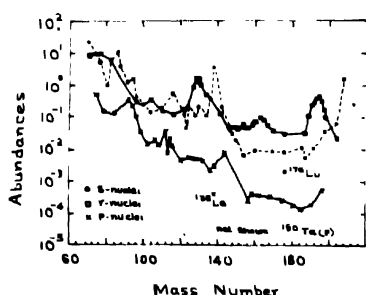


Figure 1. The solar system abundance of r-nuclei, s-nuclei and p-nuclei relative to $\text{Si} = 10^6$. Only isotopes for which 90% or more of the inferred production comes from a single process are shown. The data are from Anders and Gievers [13] and Käppeler *et al* [14] (from ref [7]).

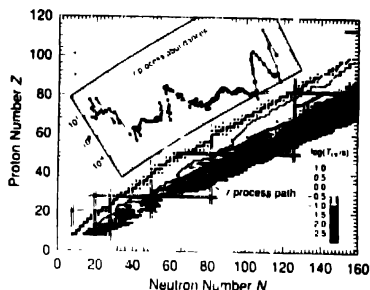


Figure 2. Schematic illustration of the r-process path (dark line on neutron rich side of beta stability) and observed r-abundances (in set). Sharp peaks occur near $A = 80, 130$ and 195 where the r-process path crosses the $N = 50, 82$ and 126 magic numbers. The chart of neutron rich nuclides is shaded according to measured (near stability) and predicted beta decay half lives ($T_{1/2}$). Gray scales for $T_{1/2}$ ranges are explained in the legend bar (This Figure from ref. [20]).

distribution with peaks around the mass numbers 87, 138 and 208. The r-nuclei, produced by rapid neutron capture process, abundance distribution shows peaks at the mass numbers 80, 130 and 195. Here it should be mentioned that the p-nuclei, *i.e.* the more proton-rich heavy isotopes produced in p-process, are not produced by neutron capture.

Earlier, we have discussed the possible neutron capture path for s-process (see Figure 3. in paper I). At the s-process branching the rate of neutron capture is comparable to the rate of beta decay. Particularly at ^{63}Ni , ^{79}Se and ^{85}Kr , the competition between these neutron capture and beta decay processes is so high that the branching of the synthesis path is determined by the s-process neutron density and the respective beta decay.

The r-process occurs in a high neutron density environment where neutron captures are faster than beta decays. In this case the overall shape of r-process abundances as well as the position of the peaks is dependent on the superposition of neutron densities [4,15–20]. The abundance distribution peaks in the $A \approx 80$ and $A \approx 130$ regions can be analyzed with the improved Solar r-process abundances by considering the steady flow and an equilibrium (waiting point approximation) between neutron captures and photo-disintegration *i.e.* $(n, \gamma) \rightleftharpoons (\gamma, n)$ [21]. But recent analysis of a few isotopic ratios in the $A \approx 80$ and $A \approx 130$ r-process peaks suggests that the above r-process abundances originate from a high density and high temperature environment (excluding the (α, n) reactions in explosive He burning) [20].

2.1. Recent *r*-process abundances :

Figure 2 shows the line of stability and the polar *r*-abundances as a function of mass number *A* using the most recent Möller *et al* [22] mass model. The abundance flow from each isotopic chain to the next depends on beta decays while the validity of the waiting point approximation (WPA) depends on high temperature and neutron number densities of the gas [23]. Cameron *et al* [23] found that this WPA was valid for the lowest temperature and corresponding neutron number density (n_n) were 2×10^9 K and $n_n \approx 10^{20} \text{ cm}^{-3}$, respectively. The beta decay rates are governed by the half lives ($T_{1/2}$) of very rich nuclei. So the knowledge of neutron number density (n_n), temperature (*T*), nuclear masses and half life ($T_{1/2}$) would only give us the physics of a whole set of abundance as a function of mass number (*A*). Kratz *et al* [21,24,25] also suggest that in order to reproduce the solar system *r*-process abundances, at least locally in the $A \approx 80$ and $A \approx 130$ peak region, beta delayed neutron emission is also important one to be considered.

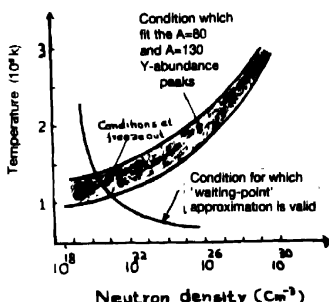


Figure 3. Neutron number densities n_n and temperature T_9 consistent with the observed *r*-process peaks (Käppeler *et al* [14]) and measured beta decay rates (Kratz *et al* [20]). Conditions for the validity of the classical waiting point approximation obtained by Cameron *et al* [23] are also shown (beyond solid line). The arrow indicates temperature and densities in an *r*-process environment before freeze out at $n_n \approx 10^{20} \text{ cm}^{-3}$ and $T = 10^9 \text{ K}$ (from ref. 20).

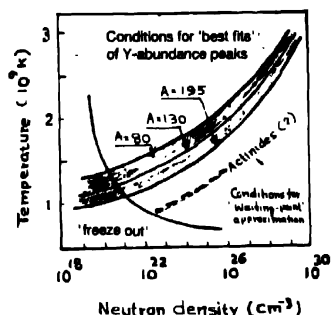


Figure 4. Illustration of the parts of the $n_n - T_9$ band which are responsible for different mass ranges of the solar *r*-process abundances. This also indicates that a superposition of at least three components is required to reproduce the $A \approx 80$ and the two mass ranges $90 \leq A \leq 130$ and $135 \leq A \leq 195$. The dashed line labelled "Actinides" only indicates a first guess (from ref. 20).

Figures 3 and 4 represent the impact on beta delayed neutron emission on the final shaping of the isotopic abundances with observed *r*-process peaks and the parts of the $n_n - T_9$ band which are responsible for different mass ranges of the solar *r*-process abundance. It is seen from Figure 3 that schematically for the *r*-process path at freeze out condition passes through and the *r*-abundance features in the range of $90 \leq A \leq 100$ occurs at $T_9 \approx 1.0 \text{ K}$ and $n_n \approx 10^{20} \text{ cm}^{-3}$. It is in good agreement [26] with the prediction of the model based on the waiting-point approximation (WPA) and a steady flow in the areas around $A \approx 80$, $90 \leq A \leq 100$ and $A \approx 130$. Within the shaded area, the solar *r*-process abundances originated from freeze-out abundances of an *r*-process, is attaining an

$(n, \gamma) \rightleftharpoons (\gamma, n)$ equilibrium with conditions $n_n \geq 10^{20} \text{ cm}^{-3}$ and $T \geq 10^9 \text{ K}$. Here, the main difficulty in such environment is, in particular, insufficient neutron production via (α, n) reaction in realistic stellar conditions [26,27]. However, using the models of Möller *et al* [28,29,22], Kratz *et al* [20] compared their results with the solar abundances and found that :

for $77 \leq A \leq 85$, the fit is very good in the r-process path before beta decay and after beta decay back to stability;

for below $A = 77$ and beyond $A = 85$, no choice of n_n gives a good fit; for $A \approx 195$, the best fit is obtained with $n_n = 3.0 \times 10^{22} \text{ cm}^{-3}$ and $T_9 = 1.2$ with a requirement of neutron density higher by two orders of magnitude.

For the whole region between $A \approx 130$ and $A \approx 195$ with the above $n_n - T_9$ conditions, they also found some local deficiency around $A \approx 142$. Finally they got three steady flow regions : $77 \leq A \leq 85$, $90 \leq A \leq 133$ and $135 \leq A \leq 195$. According to Kratz *et al* [30] nuclei below $A = 77$ seem not to originate from r-process conditions but in this region the differences of solar abundances and s-process contributions must result from a type of neutron rich freeze-out of explosive Si burning [31,32].

The peaks for $A \approx 80$, $A \approx 130$ and $A \approx 195$ in the $n_n - T_9$ plane are shown in Figure 4 labelled by $A \approx 80$, $A \approx 130$ and $A \approx 195$, respectively. They also found that their used values in the above conditions are very close to the $(n, \gamma) \rightleftharpoons (\gamma, n)$ freeze-out conditions. But for the nuclei beyond $A \approx 200$ there still remains uncertainty in conditions which reproduces such nuclei. Final r-process paths are shown in Figure 5 for the above four different r-process components. Three different r-process paths arise for the individual peaks $A \approx 80$, $A \approx 130$ and $A \approx 195$. Kratz *et al* also found that under the best fit in a local steady flow approach, the time scales for reaching the appropriate peaks are comparable and most of the time is spent in the kinks of the r-process path at magic neutron numbers for the given $n_n - T_9$ conditions. The top path for $A \approx 80$ peak reached $z = 30$ while the $A \approx 130$ and $A \approx 195$ peaks maximum for $z = 48$ and 69 , respectively. The nuclei beyond the top of each kink have longest half-lives (for example, $^{131}\text{In}_{49}$ and $^{134}\text{Sn}_{50}$ in the case of $A \approx 130$ peak) and thus form the strongest bottleneck in the r-process flow.

3. An overview of earlier problems

3.1. Star formation :

Theoretical calculations [33,34] and observational evidences, in particular the discovery of Technetium (Tc) in stars [35–41], suggest that stars form by contraction of interstellar clouds of gas and dust found in Galaxy. Such clouds are in fact, predominantly made of neutral hydrogen and typical densities in such regions are around $10^{-19} \text{ kg m}^{-3}$ (i.e. about 10^8 hydrogen atoms per cubic meter). The temperature of these regions are 100 K . At the beginning the gravitational field of such clouds of gas is unable to induce contraction because of much matter contains in it. Thermal radiative emission takes place whenever the interstellar dust grain becomes slightly heated due to collision with hydrogen atoms. By

losing its kinetic energy, the gas falls towards the centre of the cloud through gravitational attraction. As a result the gas gains some kinetic energy due to infall and then transfers some of this to the dust grains to repeat the cooling cycle. On the other hand, the atom transfers some of its centrally directed momentum to the grains. The grains then drift in towards the centre of the contracting cloud. Because of many such interactions, the clouds as a whole contract. This contraction finally produces a core of uniform density and an envelope *i.e.* an opaque core (first core) develops in which the central temperature goes up. As the central temperature is increasing a small central core (second core) appears which is almost in hydrostatic equilibrium. In these initial stages, the gravitational forces between different constituents of the object is sufficiently strong and this causes a rapid collapse of the object as a whole. This does not occur smoothly but is rather catastrophic, generating shockwaves throughout the star [42–45]. Owing to compression, heat is generated and ultimately a strong internal pressure builds up inside the star which tends to slow down the compression. This leads to the object to settle down to a more or less static state *i.e.* the pressure forces are in balance with the gravitational forces. A further increase in temperature, leads to the dissociation of H_2 and dynamical instability. The core then expands until it can radiate away, again contracts and finally accretes matter until it becomes a star. As the star contracts gradually the heat energy transportation takes place from its interior to the outer regions of the star and it develops a radiative core. However, when the temperature at the centre of the star becomes about a million degrees the first nuclear reaction sets in.

In successive stages of stellar evolution, a sequence of burning processes converts H to He, He to C and so on until the isotopes around iron are reached. The success of this nucleosynthesis depends on the atomic abundance pattern observed in nature [1,46–49]. Though these element abundances change only marginally afterwards by stellar nuclear burning, the recent direct observations of the abundance pattern in the objects like red giant, supernova remnants, interstellar matters through the advanced observation techniques suggest that the role of feedback between star and gas, physical processes and conversion of interstellar gas into star, star formation environment *etc* are very much crucial in stellar nucleosynthetic physics [50–56]. But at present, these are poorly understood.

3.2. Pre-hydrogen and hydrogen burning phase :

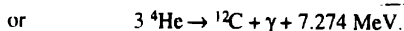
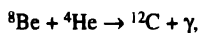
In the pre-hydrogen burning phase when temperature is $\sim 10^6$ K, the deuterium present in the contracting stellar gas begins to burn. At that time the relative abundance of deuterium is very small ($< 10^{-4}$) w.r.t. that of hydrogen. This deuterium is consumed by the reactions $D(p,\gamma) {}^3\text{He}$, $D(D,n) {}^3\text{He}$ and $D(d,p) {}^3\text{H}$ and only 0.1 neutrons per initial deuterium (*i.e.* 10^{-5} n per hydrogen atom) produced from above reactions. Of course, the presence of ${}^3\text{H}$ further reduces the number of available neutrons as it synthesizes heavy elements through the reaction ${}^3\text{He}(n,p) {}^3\text{H}$. So neutron yield contribution of the deuterium towards the heavy elements synthesis can be neglected [57].

In hydrogen burning phase the element synthesis begins with the primeval hydrogen condensed in the star through (p,p) chain reaction. In this process both (p,p) and (CNO) cycles occur. Finally, no neutron is available as yield.

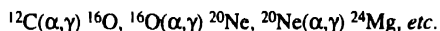
3.3. Helium burning phase :

3.3. Helium core burning phase :

Hydrogen burning in a star's main sequence stage leads to hydrogen exhaustion which then left a helium core at the star's centre. The contraction phase of the star proceeds to helium burning. The reactions are :



These reactions are assigned to the triple alpha process. This fusion of helium, according to Salpeter [58,59] and Opik [60,61], plays an important role in energy generation as well as in element synthesis in the red giant phase of the star's evolution. On the other hand, Hoyle and Schwarzschild [62] suggested that the above processes occur at the late stage of the evolution of red giant phase, in particular, when hydrogen in the central core of the star has been largely converted into helium and the central temperature rises to 10^8 K due to gravitational contraction i.e. when the helium core becomes hot enough ($\sim 1.5 \times 10^8$ K) and dense enough ($\sim 5 \times 10^4 \text{ g cm}^{-3}$) [63]. Even though the equilibrium concentration of ${}^8\text{Be}$ is very small but this amount is sufficient to lead to considerable production of ${}^{12}\text{C}$ through radiative alpha particle capture by the ${}^8\text{Be}$ [64,65] as well as of ${}^{16}\text{O}$, ${}^{20}\text{Ne}$, etc by succeeding alpha particle captures :



Although it seems that this radiative alpha capture process might continue indefinitely but the process of formation of ${}^{16}\text{O}$ through the radiative alpha capture by ${}^{12}\text{C}$ is a very slow process, except in very massive stars and at very high temperature [66]. This means that helium is built mainly into ${}^{12}\text{C}$ and ${}^{16}\text{O}$, in relative amounts that depend on the relative cross sections of the triple alpha reaction and ${}^{12}\text{C}(\alpha, \gamma) {}^{16}\text{O}$ reaction.

In the determination of the role of the triple alpha reaction the excited state of ${}^{12}\text{C}$ and Q value [$= ({}^{12}\text{C}^{**} - 3 {}^4\text{He}) c^2$] of the triple alpha reaction are important. Earlier calculations (both theoretically and experimentally) for the excitation energy of the ${}^{12}\text{C}$ excited states [67–79] and for the Q values [80–84] suggest the values of excitation energy of ${}^{12}\text{C}$ excited state and Q value are $(7654.07 \pm 0.19) \text{ KeV}$ and $(379.38 \pm 0.20) \text{ KeV}$, respectively. While direct measurement [85] indicates $Q = (379.6 \pm 2.0) \text{ KeV}$ with an uncertainty in the triple alpha rate of only about 1% at temperature $T = 2 \times 10^8 \text{ K}$.

Regarding measurement of reaction cross section of ${}^{12}\text{C}(\alpha, \gamma) {}^{16}\text{O}$, various models of reaction mechanism like R-matrix model [86,87] with two 1^- states at 7.1 MeV, 9.6 MeV

and a fictitious 1^- state at higher energies; K-matrix model [88], and Hybrid R-matrix potential model [89] have been considered. The hybrid model gives the reaction S-factor as

$$S = 0.008 + 0.05 \\ - 0.04$$

with small error which agreed with those values obtained from other models, although they have large uncertainties in their obtained values.

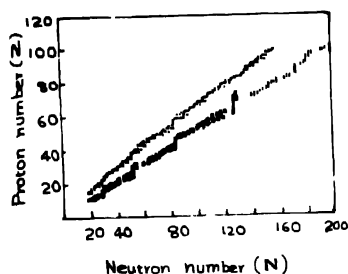


Figure 5. The final r-process path of all four components. Open squares are for components 1 and 3 (going slightly beyond $N = 50$ and $N = 126$), solid squares for components 2 and 4 (upto $N = 82$ and beyond $N = 126$) i.e. there is not one unique r-process path which reproduces the whole solar abundance curve (from ref. [20])

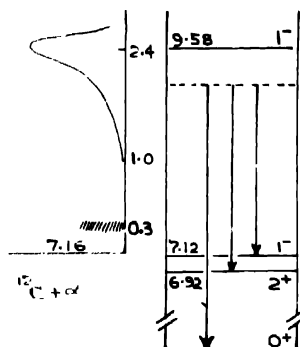


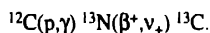
Figure 6. Schematic cross section of the $^{12}\text{C}(\alpha, \gamma) ^{16}\text{O}$ reaction obtained by Barker [90] and energy level diagram of ^{16}O

Barker [90] has also measured the low energy cross section of the $^{12}\text{C}(\alpha, \gamma) ^{16}\text{O}$ reaction at the energy of 0.3 MeV (the effective interaction energy at which astrophysical S-factor is calculated [91,92]) using the R-matrix formulae which includes the cascade transitions for the $^{12}\text{C} + \alpha$ d-wave phase shift [93]. His measurement was concentrated at the value obtained by Munster group [94] and Caltech group [95] i.e. from cross section's peak at $E_{\text{cm}} \approx 2.4$ MeV ($\sigma \approx 50$ nb), i.e. the peak corresponds to the 9.58 MeV, 1^- level of ^{16}O with 0^+ as ground state, down to $E_{\text{cm}} \approx 1$ MeV ($\sigma \approx 0.20$ nb). It has been found that the range of S-factor i.e. $S(0.3)$ values obtained by Barker (see Figure 6) are large compared to the presently accepted values. The probable reasons are due to consideration of

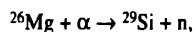
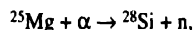
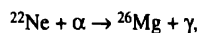
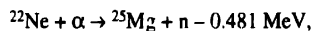
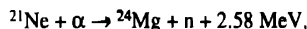
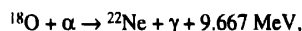
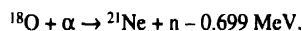
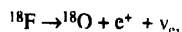
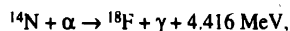
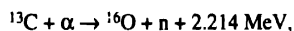
- transition because of isospin mixing in the 9.58 MeV level;
- expected subthreshold 7.12 MeV, 1^- level and 6.92 MeV, 2^+ level, and their ghosts [96];
- observation of cascade γ -transitions [94] through the above mentioned two levels i.e. 7.12 MeV and 6.92 MeV levels.

3.3.2. Production of ^{13}C :

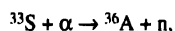
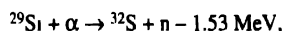
It is believed that during helium burning approximately equal amounts of ^{12}C and ^{16}O are produced in the stars of mass range $0.5 - 50 M_{\odot}$. As soon as ^{12}C is formed alpha capture process will become active and the reactions of CNO cycle produce neutrons [14,97–99]. But von Weizsacker [97] predicted that additional production of ^{13}C is crucial. When ^{12}C , produced in helium burning, is mixed with hydrogen at high enough temperature the conversion of hydrogen into helium by C–N cycle might produce ^{13}C through the following reaction



That ^{13}C produced in the C–N cycle, can act as a source of neutrons [100–104] as well as other particles :



and special cases [5]



i.e. dominant neutron producing reactions are $^{13}\text{C}(\alpha,n) ^{16}\text{O}$, $^{18}\text{O}(\alpha,n) ^{21}\text{Ne}$, $^{21}\text{Ne}(\alpha,n) ^{24}\text{Mg}$, $^{22}\text{Ne}(\alpha,n) ^{25}\text{Mg}$, $^{25}\text{Mg}(\alpha,n) ^{28}\text{Si}$, $^{26}\text{Mg}(\alpha,n) ^{29}\text{Si}$. In the above it is also noticeable that

- heavy elements ($A > 65$) are synthesized in red giant stars by slow neutron capture process,
- (α,n) reactions provide neutrons required for this,
- ^{13}C and ^{22}Ne take part in major reactions in alpha capture process.

Concerning the $^{13}\text{C}(\alpha,n) ^{16}\text{O}$ reaction, it is considered one of the main neutron producing reactions or neutron sources [100,101,105–107] in helium burning phase and the rate of this

exothermic reaction $^{13}\text{C}(\alpha, n) ^{16}\text{O}$ at stellar energies seems to be well enough [108–110]. But the main difficulty arises from the fact that at equilibrium in the C–N cycle,

- (i) only a small amount of ^{13}C is produced (*i.e.* $^{13}\text{C}/^{12}\text{C} = 1/4.6$ by number at equilibrium) and
- (ii) the most abundant isotope is ^{14}N .

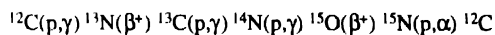
As the $^{13}\text{C}/^{12}\text{C}$ by number at equilibrium is very small, only a few neutrons are available when ^{13}C begins to react with the helium. Again cosmic abundance ratio $^{12}\text{C}/^{56}\text{Fe} = 6.4$ implies that 1.4 neutrons, which are sufficient to build nuclei slightly heavier than ^{56}Fe , will be available. Here main difficulty arises due to consideration of $^{14}\text{N}(n, p) ^{14}\text{C}$ because of isotopic abundance of ^{14}N at equilibrium in the C–N cycle. This reaction consumes a large fraction of the neutron produced in the $^{13}\text{C}(\alpha, n) ^{16}\text{O}$ reaction.

3.3.2.1 Hot C–N–O cycle and non-standard mixing :

To avoid above difficulties Cameron [111] emphasized that the $^{13}\text{C}(\alpha, n) ^{16}\text{O}$ reaction becomes dominant neutron source provided a considerable mixing between core and envelope takes place in star's giant phase. If so, then hydrogen from the envelope interacts with ^{12}C (produced from $3 ^4\text{He} \rightarrow ^{12}\text{C}$) in the core and maintains constant supply of ^{13}C at such a rate that a little ^{14}N is produced through $^{13}\text{C}(p, \gamma) ^{14}\text{N}$. The important points are :

Firstly, if ^{12}C is mixed with the cooler outer regions of the core where ^{13}C is burning, then ^{12}C captures the protons released by the reaction $^{14}\text{N}(n, p)$ and ultimately replenishes the ^{13}C *i.e.* evaluation of $^{12}\text{C}/^{13}\text{C}$, $^{12}\text{C}/^{14}\text{N}$, and mixing of chemical compositions are very much crucial. Recent evaluation of $^{12}\text{C}/^{13}\text{C}$ for the low and intermediate mass stars in the red giant branch by Charbonnel [112] as well as its comparison with the standard stellar models [113–118] indicates that the ratio $^{12}\text{C}/^{13}\text{C}$ at the stellar surface is constant during the main sequence phase and decreases abruptly at the beginning of the ascent of the red giant phase of stars with masses 1–7 M_{\odot} . At the end of the first dredge-up phase, this ratio $^{12}\text{C}/^{13}\text{C}$ varies as a function of the initial stellar mass for different metallicities. Similarly, in case of surface ratio $^{12}\text{C}/^{14}\text{N}$, the value of it decreases with the increasing depth of the external convection zone. At the end of the first dredge-up, the final surface ratio $^{12}\text{C}/^{14}\text{N}$ decreases with increasing stellar mass and decreasing metallicity for higher stellar metallicities (*i.e.* $z = 0.040, 0.020, 0.008$) while for low stellar metallicities ($z = 0.004, 0.001$) with stellar mass $> 2.5 M_{\odot}$, the surface ratio $^{12}\text{C}/^{14}\text{N}$ behaves in the reverse manner. On the other hand, theoretical calculations predict that the efficiency of the first dredge-up to change the ratio of $^{12}\text{C}/^{13}\text{C}$ at the surface depends on both stellar mass and metallicity [119,120] and observations of C–N–O elements in various evolved stars [121,122] open galactic clusters [123–125] and globular clusters [126–128] pointed out that observed surface ratios of $^{12}\text{C}/^{13}\text{C}$ and $^{12}\text{C}/^{14}\text{N}$ are substantially lower than theoretical predicted post dredge-up ratio. The origin of these discrepancies may be due to extra mixing in evolutionary phases *i.e.* turbulent diffusion mixing on the main sequence phase [129], meridional circulation on the main sequence [120] or on red giant phase [130]

or after first dredge-up some transport processes occur in the deep interior of these stars on red giant as well as several uncertainties and constraints [112] both appeared during the evolutionary phase. Secondly, we discuss the possibility of development of the 'hot' C-N-O- cycle [131]. During hydrogen burning the conversion of hydrogen into helium can occur through the 'cold' CNO cycle



and generation of energy can be limited due to the slowest reaction $^{14}\text{N}(\text{p},\gamma) ^{15}\text{O}$. But the scenario changes with increasing temperature and densities. Under increased temperature or densities the cold CNO cycle can shift to the hot CNO cycle where the reaction $^{13}\text{N}(\text{p},\gamma) ^{14}\text{O}$ bypasses the beta-decay of ^{13}N (because of slow beta decays of ^{14}N and ^{15}O). Not only that, the rate of $^{13}\text{N}(\text{p},\gamma) ^{14}\text{O}$ reaction also influences the number of available neutrons in the stellar environment produced from the $^{13}\text{C}(\alpha,\text{n}) ^{16}\text{O}$ reaction as well as the efficiency of the synthesis of heavy elements ($> ^{56}\text{Fe}$) by neutron captured [132]. Various direct [133] and indirect [134] measurements show that at temperature $T \geq 10^8$ K the reaction rate of $^{13}\text{N}(\text{p},\gamma) ^{14}\text{O}$ is dominated on the first 1^- excited state of ^{14}O at 5.173 MeV with a total width $\Gamma = 38.1 \pm 1.8$ MeV [135,136] and a partial γ width $\Gamma_\gamma = 3.8 \pm 1.2$ MeV [137]. The $^{13}\text{C}/^{12}\text{C}$ abundance ratio calculated from the above, appears to be about 30–40% lower with the LLN rate [133] than the presently accepted CF88 rate [92]. This means that measurement of the exact $^{13}\text{N}(\text{p},\gamma) ^{14}\text{O}$ rate is crucial in order to evaluate the exact role of the $^{13}\text{C}(\alpha,\text{n}) ^{16}\text{O}$ reaction in giant phase.

3.3.3 Production of ^{21}Ne , ^{22}Ne as an alternative :

Due to the above discrepancies, Fowler *et al* [138] proposed $^{21}\text{Ne}(\alpha,\text{n}) ^{24}\text{Mg}$ reaction as an alternative neutron source in helium burning phase. According to them, in the hydrogen shell burning at about $30\text{--}50 \times 10^6$ K ^{20}Ne , produced in the helium burning phase, is converted into ^{21}Ne through the reaction $^{20}\text{Ne}(\text{p},\gamma) ^{21}\text{Na}(\beta^+, \nu_e) ^{21}\text{Ne}$ and that ^{21}Ne then produces neutrons by interacting with helium *i.e.* $^{21}\text{Ne}(\alpha,\text{n}) ^{24}\text{Mg}$ satisfying some conditions like :

production of ^{21}Ne from the reaction $^{20}\text{Ne}(\text{p},\gamma) ^{21}\text{Na}(\beta^+, \nu_e) ^{21}\text{Ne}$ is faster than the production of ^{22}Na from the reaction $^{21}\text{Ne}(\text{p},\gamma) ^{22}\text{Na}$; conversion of ^{20}Ne into ^{21}Ne will not occur before hydrogen is exhausted by C-N cycle; at low temperature fairly well scoured out of ^{14}N before ^{21}Ne begins to interact, *etc.* In this context, Ulrich [139] and Iben [140] indicated that both the reactions $^{13}\text{C}(\alpha,\text{n}) ^{16}\text{O}$ and $^{22}\text{Ne}(\alpha,\text{n}) ^{25}\text{Mg}$ are the most important neutron sources in the helium burning phase in the astrophysical s-process.

Meanwhile, the measurements of the reaction rate of $^{13}\text{C}(\alpha,\text{n}) ^{16}\text{O}$ and $^{22}\text{Ne}(\alpha,\text{n}) ^{25}\text{Mg}$ reactions in the energy region of helium burning shell and stellar reaction rate suggest that $^{22}\text{Ne}(\alpha,\text{n}) ^{25}\text{Mg}$ is the most favourable neutron source [141] with a negative Q value $Q = -0.482$ MeV. Considering $^{22}\text{Ne}(\alpha,\text{n})$ reaction as a primary neutron source in this stage and experimental data above the laboratory energies $E_\alpha = 1.9$ MeV Caughlan *et al* (CFHZ) [142] then evaluated the reaction rate of $^{22}\text{Ne}(\alpha,\text{n}) ^{25}\text{Mg}$ reaction. But problem arises from

the behaviour of ^{22}Ne as neutron poison (via the $^{22}\text{Ne}(n,\gamma)$ reaction) at the same time. However, recent studies [143–148] of the reaction rate of the above two nuclear reactions with the help of advanced ion beam techniques surprisingly suggest that $^{13}\text{C}(\alpha,n)^{16}\text{O}$ as well as $^{22}\text{Ne}(\alpha,n)^{25}\text{Mg}$ is a possible neutron source in this stage. Here, Raiteri *et al* [149] raised an argument that in the low mass star ascending the Asymptotic Giant Branch the major neutron source is $^{13}\text{C}(\alpha,n)^{16}\text{O}$, not the $^{22}\text{Ne}(\alpha,n)^{25}\text{Mg}$ reaction. In order to determine the exact role of the above two alpha capture reactions as neutron source, the assessment of neutron balance [150–152], origin of the resonance at 623 KeV to $^{22}\text{Ne}(\alpha,n)^{25}\text{Mg}$ reaction [153], accurate measurement of low energy (α,n) cross section [154] are very much essential.

3.4. Carbon and oxygen burning :

At the end of helium burning the predominant nuclei are ^{12}C and ^{16}O . The dominant neutron producer, according to Arnett and Thielemann [155] and Cameron [111], is the $^{13}\text{C}(\alpha,n)^{16}\text{O}$ reaction. From the study of carbon core burning of massive stars at higher temperature ($> 8 \times 10^8$ K), Arcoragi *et al* [156] found that $^{21}\text{Ne}(\alpha,n)^{24}\text{Mg}$ is the efficient neutron producer as $^{22}\text{Ne}(\alpha,n)^{25}\text{Mg}$ at one point or another in the carbon burning layer, while $^{25}\text{Mg}(\alpha,n)^{28}\text{Si}$ is, by far, least effective. They also found the neutron production efficiency of the $^{13}\text{C}(\alpha,n)^{16}\text{O}$ reaction could be reduced drastically if the production of ^{13}C (via $^{12}\text{C}(p,\gamma)^{13}\text{N}(\beta^+)^{13}\text{C}$) can be counter balanced to large extent by ^{12}C (through $^{14}\text{N}(\gamma,p)^{12}\text{C}$).

3.5. Influence of new rates :

In the above we see that in alpha capture reaction ^{13}C as well as ^{22}Ne play an important role for production of neutrons. The evaluated values of reaction rates of ^{13}C and ^{22}Ne by Caughlan and Fowler (CF88) [92] and Beer and Voss [157] are widely accepted. During the investigation of the reaction rate of ^{13}C and ^{22}Ne in alpha capture processes Meynet and Arnould [158] have recently used a new set of rates (called new rates) instead of existing rate CF88. These new rates give many interesting results, some of which are discussed below :

3.5.1. He core burning :

Using the 'New rates' Meynet and Arnould [158] found that a burst of neutrons are available in two stages during He core burning. A first burst of neutrons occur at the beginning of He burning when ^{13}C is rapidly consumed by the reaction $^{13}\text{C}(\alpha,n)^{16}\text{O}$. Due to rapid consumption of ^{13}C , ^{14}N becomes active as a large abundance and finally this ^{14}N converted into ^{22}Ne via

$^{14}\text{N}(\alpha,n)^{18}\text{F}(e^+,v)^{18}\text{O}(\alpha,\gamma)^{22}\text{Ne}$. That ^{22}Ne , it seems, keeps a roughly constant abundance during most of the helium burning phase and gives a second burst of neutrons

through the alpha capture reaction $^{22}\text{Ne}(\alpha, n) ^{25}\text{Mg}$. This second burst is more important in the sense that

- (i) availability of ^{22}Ne is about two orders of magnitude higher than that of ^{13}C .
- (ii) strongly peaked and 80% of the total neutron expose occur near the end of central He burning,
- (iii) an increase by 50% of the burning time of ^{22}Ne at He exhaustion. Because of the competing reaction $^{22}\text{Ne}(\alpha, \gamma) ^{26}\text{Mg}$ this 50% increase contributes only a 30% rise in the total neutron exposure.

So modifications (with the new rates) in the reaction rates of both $^{22}\text{Ne}(\alpha, n) ^{25}\text{Mg}$ and $^{22}\text{Ne}(\alpha, \gamma) ^{26}\text{Mg}$, have influence on neutron production. At higher temperature $T < 2.4 \times 10^8$ K, the quantity of neutrons liberated from $^{22}\text{Ne}(\alpha, n) ^{25}\text{Mg}$ is 1.5–3.2 times more than that of from CF88 although the new rate for $^{22}\text{Ne}(\alpha, n) ^{25}\text{Mg}$ is smaller than the CF88 rate at that temperature [8, 158, 159]. Even with the new rate the modified reaction rate of $^{18}\text{O}(\alpha, \gamma) ^{22}\text{Ne}$ reaction influences the ^{22}Ne abundance [160]. Main difficulties arise from recent experiments also. Using the parameters obtained by Wiescher *et al* [160], Baraffe and El Eid [8] found in an experiment that the new reaction rate of $^{22}\text{Ne}(\alpha, n) ^{25}\text{Mg}$ is higher than the CF88 rate by a factor of the order of 100 at temperature $T \sim 1.5 \times 10^8$ K which has a very small influence on the ^{22}Ne abundance or neutron production. While in another experiment the absolute highest value of the new reaction rate of $^{22}\text{Ne}(\alpha, n) ^{25}\text{Mg}$ at temperature $T = 0.2\text{--}0.3 \times 10^9$ K, as obtained by Drotleff *et al* [161], shows higher by a factor of 70 than the CF88 rate. Due to the dependence of reaction rate of $^{22}\text{Ne}(\alpha, n) ^{25}\text{Mg}$ on temperature [162] and the involvement of high temperature at the end of core He burning, the ratio of $(\alpha, n)/(\alpha, \gamma)$ reaction rate at high temperature is also very much important to understand the effects on neutron production.

Another important new reaction rate which affect neutron production is the isotopic ^{21}Ne and ^{17}O , ^{18}O . The s-factor measurements of $^{21}\text{Ne}(\alpha, n) ^{24}\text{Mg}$, $^{18}\text{O}(\alpha, n) ^{21}\text{Ne}$ and $^{17}\text{O}(\alpha, n) ^{20}\text{Ne}$ [163] indicate that towards the low energies (*i.e.* below 1000 KeV) there is an increase of $^{21}\text{Ne}(\alpha, n) ^{25}\text{Mg}$ reaction rate by a factor of 1000 compared to CF88 rate (and some contribution from resonances is expected although resonances not yet obtained) and the reaction rate is smaller by a factor of 10 (without resonance contributions) than the CF88 rate. Low energy sector of the excitation function of this $^{21}\text{Ne}(\alpha, n) ^{25}\text{Mg}$ reaction needs detailed investigation with special attention particularly impurities in the gas as well as back ground reactions.

Regarding $^{18}\text{O}(\alpha, n) ^{21}\text{Ne}$ reaction, its reaction rate is in good agreement with the earlier rate calculated by Endt [164] but at lower temperature it is smaller by a factor of 10 than the CF88 rate. Similarly for $^{17}\text{O}(\alpha, n) ^{20}\text{Ne}$ reaction, the reaction rates are lower by a factor of 100 compared to CF88 rate at lower temperature while at higher temperature ($T > 0.5 \times 10^9$ K) it is in good agreement with CF88 rate.

3.5.2. Carbon and Ne shell burning :

During carbon burning phase, the $^{12}\text{C}(^{12}\text{C}, n)^{23}\text{Mg}$ reaction is the only neutron source. In order to determine the exact contribution of this ^{12}C reaction as neutron producer, the contribution of ^{12}C in the alpha capture process via $^{12}\text{C}(\alpha, \gamma)^{16}\text{O}$ is very much essential. But the latter contribution is not fully known, because of (i) quick transformation of the synthesized nuclei as well as remaining oxygen into Si group [165–167] and (ii) carbon oxygen mixing and different available reaction rates of various isotopic oxygen abundances [167–171] as well as the strong screening the carbon ignition by oxygen ions.

In carbon burning, ^{23}Na is produced and that ^{23}Na converts into ^{26}Mg in the Ne shell burning and finally into ^{29}Si by capturing alpha particles with a release of short intense neutron burst [172, 173]. The average value of this neutron burst in the convective Ne shell, according to Sharling's recent investigation [167], decreases from $7 \times 10^{11} \text{ n/cm}^3$ down to $4 \times 10^{10} \text{ n/cm}^3$. One of the possible reasons is the coexistence of convective O-shell burning with Ne shell burning [174].

3.5.3. Oxygen shell burning :

At temperature $T \approx 2 \times 10^9 \text{ K}$ in the oxygen shell burning the main neutron source is $^{16}\text{O}(^{16}\text{O}, n)^{31}\text{S}$ and shell burning provides Si seeds for silicon burning. Electron capture during late stage of oxygen shell burning increases the neutron excess ultimately help in the formation of iron peak nuclei as end product of nuclear burning [175–181]. Observations [175] indicate that this neutron excess (due to electron capture) increases as the density increases. Unstable nuclei ^{56}Ni alongwith new decay products are also available simultaneously. This creates fluctuations of abundance of ^{16}O in the gradient region which in turn gives troubles for determining the exact nature of oxygen shell burning.

4. Recent progress

4.1. Star formation .

Earlier we have discussed that the star formation environment, where conversion of interstellar gas into stars takes place, plays an important role in understanding stellar nucleosynthetic physics. The interstellar gas clouds or the molecular gas clouds are mainly composed of molecular hydrogen which are dense and very cold. During star formation, the basic formation process involves the gravitational collapse of molecular cloud fragments. Recent analysis [182–185] of star formation regions, indicates that most of the molecular gas is in the form of giant cloud complexes, having internal number densities $\sim 10^3 \text{ cm}^{-3}$ and diameter $\sim 100 \text{ pc}$. The average gas surface densities *i.e.* the molecular and atomic surface densities each separately has a special role on the disk average (*i.e.* averaged over the optical diameter of the disk) star formation rate, particularly on the average H_α disk surface brightness. The ultra-violet surface brightness measurements also show the dependence on the average total H_2 and HI surface densities, although the coupling between the star formation rate and molecular surface density is surprisingly weak [186–189]. But the problem arises due to the earlier observations [190, 191] which show a strong correlation

between the star formation rate and HI surface density (even though HI small) and raised a question of the dependence of the HI density (*via* photo-dissociation of molecular hydrogen) on the star formation rate or *vice versa*.

Kennicutt *et al* [192] recently study the correlation between H_α surface brightness and HI column density in cells of 220 pc in the LMC and found that cloud formation/denstruction process is one of the most important factor to determine the star formation efficiency in the star formation region where internal cloud processes dominate. In the active star forming region, the thresholds occur at surface densities $\sim 10^{21} \text{ H cm}^{-2}$ with a significant variation between galaxies. But VLA observation [193] suggests that galaxies exhibit large spatial variation in HI density. This means that possibility of other threshold mechanism in the critical densities cluster near $10^{21} \text{ H cm}^{-2}$. Another important factor arises regarding the behaviour of molecular gas formation/gravitationally bound cloud formation as a crucial regulator of star formation *i.e.* which one, whether molecular gas formation or gravitationally bound cloud formation, controls, the star formation rate is still unknown.

Again from numerical simulations and model calculations [194–196] on star formation rate and disk evolution, it is understood that under the influence of self gravity, gas cooling *etc.*, the star formation rate becomes more rapid than the observed one. So, gas density, growth rate of clouds are very much important not only for star formation rate but also for nuclear reaction rate next to the beginning of nuclear reaction for stellar evolution.

For understanding its infrared and submillimeter observations of the proto-star objects have been done [197–200] and still going on but the true evolutionary scene of the protostar is not yet fully known [201,202]. Main uncertainty in the protostar arises due to missing link between the dense molecular cloud cores and embedded premain sequence stars. As a result, how much portion of the molecular cloud collapses to form a star is not certain.

4.2. Abundances :

During helium burning s-process alpha capture processes produce neutrons, a part of which is used to initiate next stage neutron capture reactions and this chain continues till the formation of Fe core of a massive star. In the supernova phase the s-process (slow) changes its direction to r-process (rapid). Various r-process mechanisms have considered depending upon different locations (*i.e.* neutron density, time scale, *etc.*) [203–210] within the supernova. In this stage exact neutron density is very much important because this excess neutrons will characterise the initial matter and raise the ratio of neutron to seed nuclei [4,211,212]. This large ratio may finally stimulate r-process. Recently, Woosley *et al* [213] have investigated the behaviour of neutron number density and temperature during the time evolution of r-process phase of nucleosynthesis (see Figure 7). They choose only 40 mass points considering the hot bubble model [214] and mixing length convection model [212] alongwith the r-process network procedure followed by Meyer *et al* [207]. At temperature $T_9 = 2.5$ (*i.e.* $2.5 \times 10^9 \text{ K}$) they began their calculation for the trajectory of each of the 40 mass points and ≈ 0.31 second just after the material lifts off the surface of the neutron star

i.e. evolution of materials along the same trajectories is from $T_9 = 2.5$ to that point where all of the neutrons have been captured. They found that the neutrons to seed ratio for trajectory 40) at $T_9 = 2.5$ is 77 under the consideration that the seed nuclei for neutron capture in the r-process to be all nuclei other than ${}^4\text{He}$. This obtained ratio is higher than that of Meyer *et al* which means that the possible product nuclei are of $A \geq 200$. Figure 8 shows the final

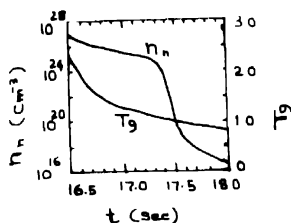


Figure 7. The behaviour of neutron number density and temperature against time evolution for the r-process phase of nucleosynthesis as obtained by Woosley *et al* [213]. The r-process phase calculation begins at temperature $T_9 = 2.5$ (from ref. [213]).

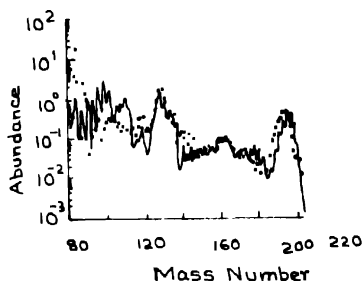


Figure 8. Final mass weighted r-process abundances (line) as a function of atomic mass, obtained by Woosley *et al* [213], comparing with the solar r-process abundances (points) of K  ppler *et al* [14] (from ref. [213]).

mass weighted r-process abundance distribution coupling with the solar r-process abundance distribution of K  ppler *et al* [14]. It has been found that at the beginning of r-process only fewer neutrons per seed nucleus (thus fewer heavy nuclei produced) are produced by the trajectories which contribute to the r-process abundance peak at $A \sim 130$ or below, while at the later stage, a large number of neutrons per seed nucleus gives a strong abundance peak at $A = 195$. After normalizing all the calculated parameters with reference to the fixed abundance-peak isotopes (i.e. ${}^{129}\text{Xe} = 1.21 [{}^{29}\text{Si}] \times ({}^{129}\text{Xe}) = 3.95 \times 10^{-9}$), they found that all of the r-process isotopes are within a normalization band which is about 10 times the solar abundance. This value is in good agreement with the models calculated from the average of every supernova but problem arises for supernovae from low mass progenitor stars which are less efficient for producing the heavy r-process nuclei. Not only that, the explanation of the shift in the $A = 195$ peak by a couple of mass units and the over production of $A \approx 180$ nuclei also posed difficulties in their investigation. Of course, there are some evidences [207] that lower mass supernovae may be some of the possible dominant contributors to r-process abundances. However, more investigations [215,216] are needed for understanding the heavy nuclei abundance of r-process nucleosynthesis.

4.3. Helium burning :

It is believed that in helium burning phase alpha capture process becomes active as soon as ${}^{12}\text{C}$ is formed and this finally produces ${}^{13}\text{C}$ when it is mixed with hydrogen at high temperature *vide* the reaction ${}^{12}\text{C}(p,\gamma) {}^{13}\text{N}(\beta^+, \nu_e) {}^{13}\text{C}$. As ${}^{13}\text{C}$ formed in the CNO cycle acts as a source of neutrons (as well as other particles) the reaction cross section of ${}^{12}\text{C}(p,\gamma) {}^{13}\text{N}$

is very much essential to evaluate the role of ^{13}C as neutron producer [217]. Recently, Zucchiatti *et al* [218] have studied the behaviour of $^{12}\text{C}(p,\gamma)^{13}\text{N}$ reaction in the excitation

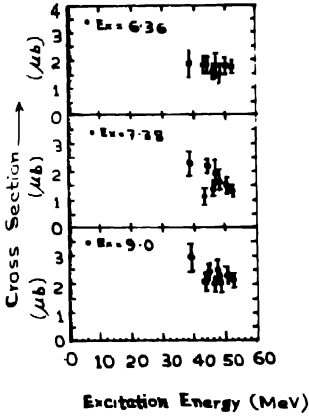


Figure 9. Total cross section for the $^{12}\text{C}(p,\gamma)^{13}\text{N}$ reaction as a function of the excitation energy (from ref [218])

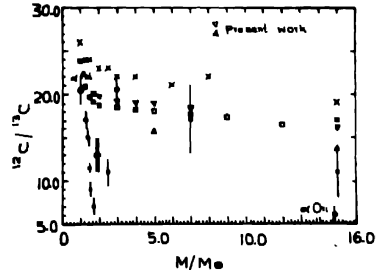


Figure 10. Variation of surface $^{12}\text{C}/^{13}\text{C}$ after the "first dredge up" phase against masses as adopted by Harris *et al* [226]. ● – observed values of M F El Eid [225]; X – predicted values of Dearborn [219]. □ – obtained by Schaller *et al* [113] (This figure from ref. [225]).

energy range 40–54 MeV (Figure 9). In their experiment, they found that no resonant decay of ^{13}N either at ground state or at excited state. But single proton is coupled to the excited ^{12}C core in the excited states at 6.36, 7.38 and 9.00 MeV through the two step reaction mechanisms—excitation of the core followed by capture. Observed cross section for this two-step process are of the order of 1.5 to 2 μb *i.e.* surprisingly large being nearly half as big as the cross section for the direct transition. So, capture to states with an excited ^{12}C core is also another important area which needs more thorough investigation.

In this phase, another important one is the CNO isotopic abundance ratio of carbon and oxygen *i.e.* $^{12}\text{C}/^{13}\text{C}$, $^{16}\text{O}/^{17}\text{O}$ and $^{16}\text{O}/^{18}\text{O}$ [219–224]. Figure 10 shows the recent observed values (along the downwards oriented triangles) of surface $^{12}\text{C}/^{13}\text{C}$ and the predicted one. The observed values are in good agreement with the values predicted by Dearborn [219] except for two cases : α Ori star and star of mass below $3 M_{\odot}$. In case of α Ori star the observed value is extremely low which is not yet understood at all. In case of stars with masses below $3 M_{\odot}$ the observed values are so peculiar that these can not be explained only by the first dredge-up scenario because of the possible role of core helium flash or scenario of non-standard extra mixing of ^{13}C during the main sequence phase. To understand it the behaviour of oxygen isotopic ratios are very much essential [227].

Figures 11 and 12 show the observed and predicted values of oxygen isotopic ratio $^{16}\text{O}/^{18}\text{O}$ and $^{16}\text{O}/^{17}\text{O}$, respectively. In case of $^{16}\text{O}/^{18}\text{O}$ there is a good agreement between the

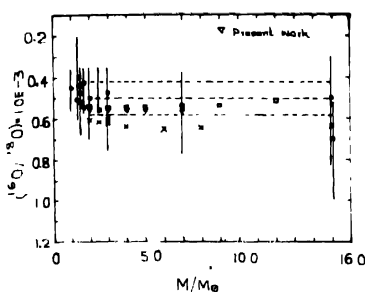


Figure 11. Comparison between the observed $^{16}\text{O}/^{18}\text{O}$ ratio and predicted values. ∇ -present observed values obtained by M F El Eid [225], \times -predicted values by Dearborn [219], \square -observed values by Schaller *et al* [113]. The dashed horizontal line represents the range of observations within a mean value 500 ± 80 obtained by Harris and Lambert [228] which is consistent with the value of 500 ± 50 found by Wannier [229] for interstellar medium (from ref [225])

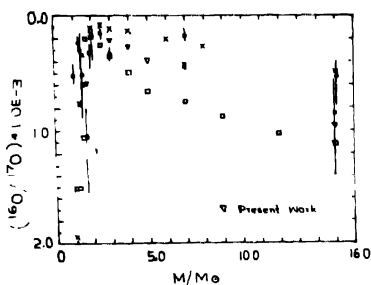


Figure 12. Behaviour of $^{16}\text{O}/^{17}\text{O}$ ratio vs mass. Others are same as to Figure 11 (from ref [225])

observed and the predicted ratio but ^{18}O seems to survive destruction, mainly by $^{18}\text{O}(\text{p},\alpha)$ ^{15}N beyond the region where ^{13}C is mostly produced [228–230]. Figure 13 represents the behaviour of resulting ratio of $^{16}\text{O}/^{18}\text{O}$ recently obtained by Boothroyd *et al* [231], considering the various values of $^{18}\text{O}(\text{p},\alpha)$ ^{15}N rate. In their investigation, it has been found that the first and second dredge-up during the star's red giant phase, contribute a minor increase in the $^{16}\text{O}/^{18}\text{O}$ ratio as the ^{18}O abundance is not altered much from its initial value during the first and second dredge-up. On the otherhand, third dredge-up gives a huge increase of the $^{16}\text{O}/^{18}\text{O}$ ratio for the AGB stars of masses $\geq 5 M_{\odot}$. Here, the remarkable point is that the ratio $^{16}\text{O}/^{18}\text{O}$ primarily depends on the initial composition of the star, not on the star mass. From the behaviour of $^{16}\text{O}/^{17}\text{O}$ it is understood that ^{17}O is produced only in deep layers of the star in a sufficiently high temperature environment. For ^{17}O there is also a high destruction of it by the $^{17}\text{O}(\text{p},\gamma)$ ^{18}F and $^{17}\text{O}(\text{p},\alpha)$ ^{14}N in massive stars. The important point is that the surface ratio $^{16}\text{O}/^{17}\text{O}$ is determined by the maximum depth of the convective envelope in the star's red giant phase *i.e.* the resulting $^{16}\text{O}/^{17}\text{O}$ and the depth of the convective envelope both depend on the stellar mass. From Figure 12 it is also seen that the observed value of $^{16}\text{O}/^{17}\text{O}$ ratio and predictions are in well agreement for the $2.0 M_{\odot}$ model. But problem arises in the cases of deviation below and above this mass. One of the possible reasons of deviation for higher masses is the selection of reaction rate of destroying ^{17}O by the resonant reaction $^{17}\text{O}(\text{p},\alpha)$ ^{14}N . Because El Eid found that the predicted values of Schaller *et al* [113] (who adopted higher rate of $^{17}\text{O}(\text{p},\alpha)$) are still higher than his obtained values although he has considered larger rates followed

by Landre *et al* [230]. For the lower masses ($< 2.0 M_{\odot}$), they found an increase tendency in the $^{16}\text{O}/^{17}\text{O}$ ratio while recent results [231] (see Figure 14) indicates that in the red giant envelope

- the $^{16}\text{O}/^{17}\text{O}$ is primarily depends on the star's mass, not on the initial composition of the star,
- uncertainties in the ^{17}O destruction rate does not have any effect on the $^{16}\text{O}/^{17}\text{O}$ ratio for the star of mass $1-2.5 M_{\odot}$;
- first dredge-up significantly decreases the value of $^{16}\text{O}/^{17}\text{O}$ ratio from the initial value;
- for the stars of masses $\geq 5 M_{\odot}$ second and third dredge-up significantly decrease the ratio $^{16}\text{O}/^{17}\text{O}$ in contrast with a huge increase in the ratio $^{16}\text{O}/^{18}\text{O}$.

Thus, we see in the above that the ratio $^{16}\text{O}/^{17}\text{O}$ significantly increases or decreases for the stars of masses $\leq 2.0 M_{\odot}$ or $1-2.5 M_{\odot}$ in the first, second and third dredge-up. The author

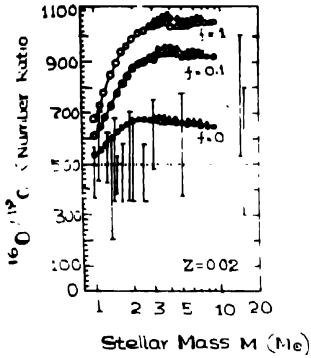


Figure 13. The behaviour of $^{16}\text{O}/^{18}\text{O}$ ratio resulting from first dredge-up (circles) and from second dredge-up (diamonds), for solar composition ($Z = 0.02$). Solid, crossed and open points show results using the CF88 rate of $^{18}\text{O}(p,\alpha)^{15}\text{N}$ reaction with destruction rate $f = 0, 0.1$ and 1 , respectively (This figure from ref [231])

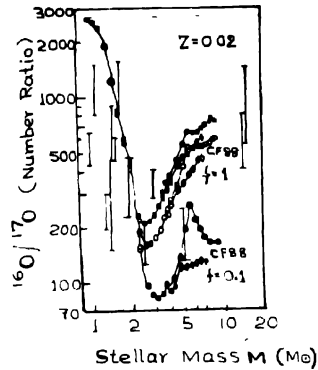


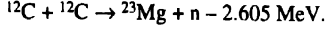
Figure 14. The ratio of $^{16}\text{O}/^{17}\text{O}$ resulting from the first dredge up (circles) and from second dredge-up (diamonds) as a function of stellar mass for the solar composition ($Z = 0.02$). Calculations were made for different reaction rates of $^{17}\text{O}(p,\gamma)^{18}\text{F}$ and $^{17}\text{O}(p,\alpha)^{14}\text{N}$. Solids for Landre *et al* [230] rate, open and cross points for the CF88 rate with $f = 1, 0.1$, respectively. Dotted line indicates the initial (solar) value of $^{16}\text{O}/^{17}\text{O}$ ratio (from ref [231])

suggests that thorough investigation of the ratio $^{16}\text{O}/^{17}\text{O}$ for the star of mass $1-3 M_{\odot}$ is needed considering all the aspects like destruction rate of ^{17}O , decrease rate of $^{16}\text{O}/^{17}\text{O}$ in each dredge-up, in each change of initial stellar masses due to change in initial compositions; *etc.* Even the $^{12}\text{C}/^{13}\text{C}$ ratio is also in the star mass $1-3 M_{\odot}$ because of extra mixing effect.

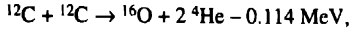
4.4. Carbon burning :

At the end of helium burning in massive stars ^{12}C and ^{16}O are available as nuclear ashes. The relative abundance of these two species depends on the yet, rather unknown reaction

$^{12}\text{C}(\alpha, \gamma) ^{16}\text{O}$. However, in the carbon core burning phase, carbon nuclei react with one another and the main neutron producing reaction is



This carbon burning also produces alpha particles :



which adds another episode of neutron producing s-process with the partial survival of ^{22}Ne at helium exhaustion for the stars of masses less than $\sim 30\ M_{\odot}$. In an investigation of the evolution of C-burning layers, Arcoragi *et al* [156] found that at temperature $> 8 \times 10^8$ K, $^{21}\text{Ne}(\alpha, n) ^{24}\text{Mg}$ reaction can be a neutron producer as the efficient as the $^{22}\text{Ne}(\alpha, n) ^{25}\text{Mg}$ reaction at one point or another in this burning phase. This result is surprising in the sense that Arnett and Thielemann [155] identified $^{13}\text{C}(\alpha, n) ^{16}\text{O}$ as the dominant neutron producing source.

This carbon burning core also suffers further nuclear processing in the later evolutionary phases because of the involvement of destruction of the s-isotopes. External carbon shell burning is one of the cause of it. This also affects the C–O core [232,233]. At very high temperature ($T_9 \sim 1$) with a high average neutron density ($\sim 10^{11}/\text{cm}^3$) the shell C burning begins. At the beginning of shell C burning the rate of $^{12}\text{C}(\alpha, \gamma) ^{16}\text{O}$ reaction is very much important for evolutionary calculations and treatment of convective mixing near the end of Core He burning [234]. Various resonances of $^{12}\text{C} + ^{12}\text{C}$ reaction near Coulomb barrier and at higher energies give another intriguing problem in the carbon burning phase. Recently, Rae and Keeling [235,236] have studied the resonance of $^{12}\text{C} + ^{12}\text{C}$ reaction at higher energy region 19–32 MeV. In their experiment, it is found that excited states of ^{20}Ne are the main contributor to the width resonances of $^{12}\text{C} + ^{12}\text{C}$ reaction. This excited ^{20}Ne is also responsible for alpha decay in this phase. They have also observed a series of resonance-like features in their experiment which need more investigation for understanding the origin of ^{12}C resonances in C-burning phase.

At the beginning of the C-burning phase, the neutron density is so high ($\sim 10^{11}\ \text{cm}^{-3}$) that a depletion of ^{63}Cu appears due to the strongly favourable situation of neutron capture by ^{63}Ni . The neutron density (n_n) controls the equilibrium abundances of ^{62}Ni , and other isotopes also. Figure 15 shows the variation of isotopic abundances of Ni, Cu and Zn in the ^{63}Ni branching against neutron density in the shell C burning in a $25\ M_{\odot}$ star. It is seen that the equilibrium abundance of ^{63}Ni does not depend on the neutron density while ^{65}Cu abundance decreases slightly because ^{64}Ni behaves as a 'Bottleneck' in the s-path due to its small neutron capture cross section. As per calculations by Raiteri *et al* [234] the weak component contributes only 30% to ^{64}Ni and s-process also gives 30% contribution to the solar abundance of ^{63}Cu and ^{65}Cu . But the problem is overproduction at a high neutron density [232]. Because the average neutron density,

mostly supplied by s-process in the core He burning in the stellar interior, never exceeds 10^6 cm^{-3} [237]. This means that ^{63}Ni (progenitor of ^{63}Cu) and ^{64}Ni are weakly produced.

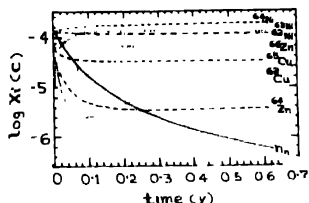


Figure 15. The isotopic abundances of Ni, Cu and Zn involved in the ^{63}Ni branching during shell C burning in a $25 M_{\odot}$ star. The neutron density (n_n) is given in units of 10^{15} cm^{-3} (from ref. 234).

So, more investigation needs on large uncertainty on the $^{12}\text{C}(\alpha, \gamma) ^{16}\text{O}$ reaction rate [238,239] as well as weak production of ^{63}Ni , ^{64}Ni , etc whether due to uncertainty in other main s-components or not.

4.5. Oxygen burning :

In massive star at temperature $\sim 2 \times 10^9 \text{ K}$, oxygen shell burning begins and it ultimately produces Si seeds for next silicon burning. The $^{16}\text{O}(^{16}\text{O}, n) ^{31}\text{S}$ is the main neutron source in this oxygen shell burning. While large electron capture in the late stage of oxygen burning produces iron peak nuclei [175–181]. This shell burning also converts ^{16}O and ^{24}Mg to the Si–Ca quasi equilibrium group *i.e.* production of neutrons in oxygen shell burning partially depends on how much electron capture reaction occurs as well as abundance of ^{16}O .

Recent investigation [240–249] on stellar oxygen abundances, indicate that the abundances of oxygen vary from star to star and there is a correlation between the neutron captured elements and the strongly variable O, and Na (produced through neutron capture synthesis) abundances. In an observation of 7774 \AA OI triplet and other oxygen lines King [242] found that the mean abundance of [O/Fe] ratio of metal poor stars is $+0.53$ with a 1σ dispersion of ± 0.12 dex. In another observation [246] King also found that the [O/Fe] ratio of a very metal poor (Fe/H ~ -3) halo star BD – 13°3442 is larger by ~ 0.35 dex than that of the other two halo stars HD 140283 and BD + 03°740. To eliminate these discrepancies in the oxygen abundance and O/Fe ratio of stellar atmosphere/interior, King and Boesgaard [247] recently investigate systematic effects on oxygen abundances derived from 6300 \AA (OI) line and 7774 \AA (OI) triplet under LTE (Local Thermodynamic Equilibrium) and non-LTE models. They also found that the discrepancy in the O abundances and O/Fe ratio still exist between the presently observed value of the oxygen abundances and O/Fe ratio and earlier observed and predicted values (*i.e.* Barbuy and Erdehji-Mendes [250], Barbuy [251], Bessell *et al* [252] [O/Fe $\sim +0.4$ to $+0.5$]; Abia and Rebolo [253] [O/Fe $\sim +1.2$]; non-LTE model calculations : Altrock [254], Lambert [255], Kiselman [256], Spiesman and Wallerstein [257] [O/Fe = $+0.3$ and 0.4]; Spite and Spite [258] [O/Fe = $+0.48$ and 0.59], etc). For LTE model their obtained value for oxygen abundance (*i.e.* $\log \epsilon(0) = 8.91$) is consistent with the presently accepted value of 8.93 and the recently determined value of 8.86 [259]. Takeda [260] has also studied the problem of non-LTE effect on oxygen abundance in metal poor stars with a special attention to oxygen

triplet λ 7771 –5. They found that the non-LTE abundance correction for oxygen abundance is fairly small (≤ 0.1 dex), and for OI triplet λ 7771 –5 is -0.06 for the sun which is smaller than those previous non-LTE calculations by 0.1 – 0.3 dex. Using the non-LTE effect of this triplet, Takeda has extended his observation to F–G popular II dwarfs also, but discrepancy in O/Fe ratio still remains.

Using new advanced hydrodynamics techniques and numerical simulation, Arnett [175], Bazan and Arnett [261] have investigated the hydrodynamic behaviour of shell oxygen burning. An abrupt change in the ^{16}O abundance occurs in the initial stage while small fluctuation (of the order of 0.05 in nuclear fraction) in the ^{16}O abundance occur at the late stage. Above the burning shell these fluctuations are much smaller. Significant composition inhomogeneity arises due to incomplete mixing of nuclear fuel from stable region toward the hotter regions of convective zone. As a result, perturbations in density, velocity, electron fraction, *etc* occur. It is observed that a 36% increase in neutron excess in this region due to the electron capture occurs as the density increases. Downdrafts sink and heat by compression creates 'hotspots' which affects the flow of fuel. The important result is that appearance of perturbation due to convection in this oxygen shell burning will enhance the mixing of ^{56}Ni nuclei. But the problem is that the unstable ^{56}Ni nuclei alongwith newly decayed products are also available as yield which is a source of trouble for accurate measurements. Although the fluctuation of abundance of ^{16}O in the gradient region is small, investigation of perturbations particularly on density perturbation, appearance of convective shell and convective flow are very crucial for understanding the exact nature of oxygen shell burning.

4.6. Supernova phase :

At the end of its nuclear fuel a massive star can become a supernova. It is believed that r-process nucleosynthesis occurs in supernova and just prior to collapse, the core of the massive star largely consists of ^{54}Fe alongwith neutron-rich isotopes like ^{48}Ca , ^{50}Ti , ^{54}Cr , ^{58}Fe , *etc* which are ashes of the silicon burning shell. Outer layers of the core consist of the ashes from the oxygen, neon, carbon, helium and hydrogen burning shells. During a supernova explosion, the temperature becomes so high ($> 4 - 5 \times 10^9$ K) within a short time scale (~ 1 sec) that transformation in the final abundances of the ejected mass takes place due to occurrence of nuclear reactions. So, if the r-process mainly occurs in the supernova explosion of massive stars, then the abundances of its products in the ejecta are functions of initial stellar metallicity *i.e.* exact estimates of abundances of heavy elements produced through s-process and r-process before the explosion and heavy element abundances after the explosion are very much important to understand the dynamics of supernova as well as after explosion evolution *i.e.* formation of dwarfs, neutron stars, *etc*. Of course, neutrinos play an active role in the explosion mechanism of massive stars while neutrino mixing creates various constraints in supernova nucleosynthesis [262,263]. In a recent study of the abundances of neutron rich elements Gratton and Sneden [166] found that the element to iron ratios for the group of elements from Ba to Eu increase with atomic number for the star

with ($-2 < \text{Fe}/\text{H} < -1$) while lighter elements (Ba, La, Ce) are slightly overdeficient by a factor of ~ 0.1 dex. In case of most metal poor stars (with $\text{Fe}/\text{H} < -2.5$) all these group of elements *i.e.* Ba to Eu are largely over-deficient with no clear evidence for a plateau at very low metallicities. Even the spread in the element to iron ratios is larger by a factor of 0.1 to 0.15 dex than the scatter the origin of which is not yet clear. Regarding solar system s-process abundance, their observed abundance pattern of neutron capture elements, particularly Ba abundance is in excess relative to solar system r-process nucleosynthesis predictions. On the other hand, observed abundance of heavy elements from s-process contribution is over estimated with respect to presently accepted solar abundances of heavy elements. This indicates that a difference exists between the observed pattern of neutron captured heavy elements (produced via s-process/r-process), and solar abundance of heavy elements as well as for metal poor stars. Only thorough investigations in this regard can give the clue to this heavy element abundance discrepancy.

4.7. Proto-neutron star phase :

At the end of final stage of the evolution of massive star, an iron core forms at the centre of the star. Due to undergoing gravitational collapse in the core, the central density reaches nuclear matter density. In this stage, the core collapses abruptly in such a manner that a 'core bounce' appears due to this. According to the present picture of prompt explosion mechanism, shock waves lose the entire kinetic energy within a very short time (few milliseconds) for stalling inside the outer edge of the initial iron core. At this moment, no disruption takes place. After a short time interval (prompt explosion) neutrino streaming coming out from the newly born neutron star. Neutron star's binding energy at this stage is so strong that it can drive a powerful shock into the overlaying stellar mantle. As a result, a matter depleted region, called 'Hot Bubble', appears which separates the central remnant and the ejected stellar envelope [264,265]. Figure 16 shows the final r-process abundances in the hot bubble region. The solid curve shows the r-process yields obtained from an integration of local values. Evaluated maximum uncertainties due to the procedure of above integration and interpolation are indicated by the shaded area. The circles with error bar represent the solar r-process abundances (normalized with the Käppeler *et al* values [14]). It has two best fit peaks of abundances of r-process nuclei (N_{\odot}, r) around the mass number $A = 130$ and $A = 195$. In the $A \leq 80$ a plateau is observed rather than an edge observed in the previous calculations [17, 267]. Previous calculations also indicate that the seed nuclei are confined to neutron rich, Fe group elements in a highly neutronized material at high temperature and high densities (because of their tendency toward NSE) while in hot bubble the seed nuclei and $A \leq 90$ are synthesized already by alpha process. This means that with the above existing discrepancies if the bulk r-process abundance of the heavy nuclei in the region $A \leq 80$ could be explained by the neutrino driven nucleosynthesis in the hot bubble phase of supernova explosion, other phases during the supernova explosion will have to be considered for complete description of solar system abundances of r-process nuclei. Figure 17 shows clearly the difference in abundances of r-process heavy nuclei when above two situations are included. The solid line represents the abundances of r-process in one

situation when beta-delayed neutron emission after the 'freeze-out' (*i.e.* when the total number of free neutrons decreases to about 1/500 of the total number of heavy nuclei) of the r-process is excluded while open circles are for the other situation where beta delayed

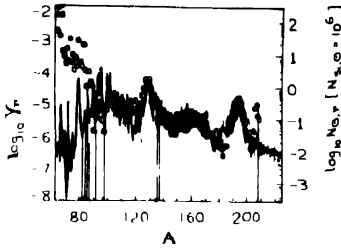


Figure 16. Final r-process abundance curve in the whole region of the hot bubble as obtained by Takahashi *et al* [266]. Solid curve represents the behavior of number fractions of r-process heavy nuclei against mass number A . The circles with error bar represent the solar r-process abundances in standard units of the Si abundance normalized to $N_{Si} = 10^6$. $N_{0,r}$ is the number of abundances of r-process nuclei in the solar system in units of $N_{0,s} \approx 10^6$. The shaded area indicates the evaluated maximum uncertainties due to the procedure of interpolation and integration (from ref. [266]).

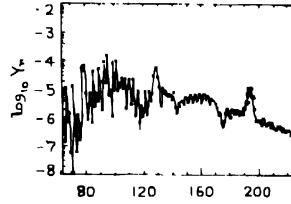


Figure 17. A comparison of the final r-process abundance curve at two different situation on Beta-delayed neutron emission after the "freeze-out" of the r-process (see text). Solid curve for the situation when beta delayed neutron emission is excluded. Open circles for the situation where beta-delayed neutron emission is taken into account (from ref. [266]).

neutron emission are considered (except reabsorption of the emitted neutrons). So, in type II supernovae neutrino wind driven hot bubble region creation gives a most promising site for r-process nucleosynthesis [268]. Not only that it also gives an initiation to search for a production mechanism of relatively light r-process nuclei ($A \leq 80$).

5. Conclusion and outlooks

We see that neutron production and its flow play an important role during various burning phases of neutron capture nucleosynthesis. New rates, hydrodynamical techniques and numerical simulations have further increased our knowledge of understanding the neutron capture nucleosynthesis. Still various difficulties and uncertainties remain for more investigation. Such as :

- How much portion of the collapsing molecular clouds form a star ?
- Non standard mixing and chemical discontinuity in hydrogen shell burning :
Theoretical calculations [112–115] indicate that a chemical discontinuity arises because of convective envelope when hydrogen burning shell reaches its maximum event. On the other hand, observations suggest that CNO element anomalies in star's chemical composition will affect the star's mass.
- Interpretation of the ratio $(^{16}\text{O}/^{18}\text{O})/(^{16}\text{O}/^{17}\text{O})$ in red giant stars [269–271] :

It should give us more insight about the combined effect of nuclear reactions and convecting mixing.

- (d) Experimental verification of the rate of $^{17}\text{O}(\text{p},\alpha)$ reaction for determining the accurate rate.
- (e) Thorough observation regarding correlation between strongly variable O and Na abundances.
- (f) Investigation of O/Fe ratio for various stars [272–274].
- (g) Inhomogeneity in composition and hotspot burning during oxygen shell burning :
These two are likely to change the details of nucleosynthesis during oxygen shell burning stage of stellar evolution.
- (h) Possibility of rotational mixing :
Recent calculations [268,275,276] indicate that the ratio of $^4\text{He}/^1\text{H}$, $^{14}\text{N}/^{12}\text{C}$ and $^{14}\text{N}/^{16}\text{O}$ are rather large at the surfaces of fully mixed star models. The possible reason of it is the rotational mixing which may cause enrichment of helium and nitrogen as well as depletion of carbon and oxygen nuclei in that star.
- (i) Measurement of screening caused by oxygen ions [277,278] during carbon shell burning.
- (j) Accurate measurements of neutron density at various burning phase and decay of Ni isotopes :
A low neutron density during core He burning in massive star favors the decay of Ni isotopes (e.g. ^{63}Ni , ^{63}Cu , ...) while high neutron density at the beginning of C burning phase causes a depletion of ^{63}Cu because of strong neutron capture by ^{63}Ni .
- (k) Search for a production mechanism of relatively light ($A \leq 80$) r-process nuclei.

Acknowledgments

The author is grateful to Petra Barkemeyer, Max Planck Institut für Astrophysik, Garching; Dr. J R King, University of Texas at Austin, USA; Library staff of JILA, Boulder, USA; Max Planck Institut für Extraterrestrische Physik, Garching, Germany; IUCAA, Pune; and NCRA, Pune, for their kind help by supplying the required preprints/reprints. He also wishes to thank Prof. H N K Sarma and Prof. P S Mazumdar, Department of Physics, Manipur University; Mrs. Tapati Parui and Rajarshree Parui for their continuous encouragement and kind help at various stages.

References

- [1] R K Parui *Indian J Phys* **67B** 109 (Paper I) (1993)
- [2] R K Parui *Indian J Phys* **69B** I (Paper II) (1995)
- [3] D D Clayton, W A Fowler, T E Hull and B A Zimmerman *Ann Phys.* **12** 331 (1961)
- [4] P A Seeger, W A Fowler and D D Clayton *Astrophys J Suppl.* **11** 121 (1965)
- [5] E M Burbidge, G R Burbidge, W A Fowler and F Hoyle ($B^2\text{HF}$) *Rev. Mod. Phys.* **29** 547 (1957)
- [6] A G W Cameron *Chalk River Rep.* **CRL41** (1957)
- [7] B S Meyer *Ann Rev Astron. Astrophys* **32** 153 (1994)
- [8] I Baraffe, M F El Eid in *Proc 7th Ringberg Conf. on Nuclear Astrophys MPA/P7* eds W Hillebrandt and E Muller (Max Planck Institute, Garching, Germany) p 75 (1993)

- [9] S E Woosley and R D Hoffman *Astrophys. J.* **395** 202 (1992)
- [10] J R Wilson and R W Mayle *Phys. Rep.* **227** 97 (1993)
- [11] S E Woosley, G J Mathews, J R Wilson, R D Hoffman and B S Meyer *Astrophys. J.* **433** 229 (1994)
- [12] S E Woosley and R D Hoffman *Astrophys. J.* **395** 204 (1992)
- [13] E Anders and N Grevesse *Geochim. Cosmochim. Acta.* **53** 197 (1989)
- [14] F Käppeler, H Beer and K Wisshak *Rep. Prog. Phys.* **52** 945 (1989)
- [15] A G W Cameron, M D Delano and J W Truran in *Proc. 1st Int. Conf. on Nuclei Far from Stability*, CERN 70-30 2 235 (1970)
- [16] T Kodama and K Takahashi *Nucl. Phys.* **A239** 489 (1975)
- [17] W Hillebrandt, K Takahashi and T Kodama *Astron. Astrophys.* **52** 63 (1976)
- [18] W Hillebrandt *Space Sci. Rev.* **21** 639 (1978)
- [19] S Gonely and A Amould *Astron. Astrophys.* (Preprint) (1992)
- [20] K-L Kratz, J-P Bitouzet, F-K Thielemann, P Moller and B Pfeiffer *Astrophys. J.* **403** 216 (1993)
- [21] K-L Kratz, F-K Thielemann, W Hillebrandt, P Moller, V Harms, A Wöhr and J W Truran *J. Phys. G* **14** 331 (1988)
- [22] P Möller, J R Nix, W D Myers and N Swiatecki *Atomic Data Nucl. Data Tables* **59** 185 (1995)
- [23] A G W Cameron, J J Cowan and J W Truran *Astrophys. Space Sci.* **91** 235 (1983)
- [24] K L Kratz, V Harms, W Hillebrandt, B Pfeiffer, F-K Thielemann and A Wöhr *Z. Phys.* **A336** 357 (1990)
- [25] K-L Kratz, H Gabelmann, P Moller, B Pfeiffer, H L Ravn and A Wöhr the ISOIDE Collaboration *Z. Phys.* **A340** 419 (1991)
- [26] J J Cowan, A G W Cameron and J W Truran *Astrophys. J.* **294** 656 (1985)
- [27] J B Blake, S E Woosley, T A Weaver and D N Schramm *Astrophys. J.* **248** 315 (1981)
- [28] P Möller, J R Nix, K-L Kratz and W M Howard in *Nuclei in the Cosmos* eds H Oberhummer and W Hillebrandt MPA/P4 (Max Planck Institute, Garching, Germany) p 226 (1990)
- [29] P Möller, J R Nix and K-L Kratz in *Proc. Int. Conf. on Exotic Nuclei* (South Crimea) in Press (1992)
- [30] K-L Kratz *et al* in *Ref. 20* p 227 (1993)
- [31] D Hartmann, S E Woosley and M F El Eid *Astrophys. J.* **297** 837 (1985)
- [32] F K Thielemann, M Hashimoto and K Nomoto *Astrophys. J.* **349** 222 (1990)
- [33] G Gamow *Phys. Rev.* **54** 480 (1938)
- [34] H A Bethe *Phys. Rev.* **55** 434 (1939)
- [35] P W Merrill *Astrophys. J.* **105** 360 (1947)
- [36] P W Merrill *Science* **115** 484 (1952)
- [37] L H Aller and P C Keenan *Astrophys. J.* **113** 72 (1951)
- [38] W Buscombe and P W Merrill *Astrophys. J.* **116** 525 (1952)
- [39] W P Bidelman *Astrophys. J.* **117** 337 (1953)
- [40] P W Merrill and J L Greenstein *Astrophys. J. Suppl.* **2** 225 (1956)
- [41] R G Teske *Publ. Astron. Soc. Pacific* **68** 520 (1956)
- [42] S Chandrasekhar *Stellar Structure* (New York : Dover) (1939)
- [43] T Kanjilal and B Basu *Indian J. Phys.* **65B** 299 (1991)
- [44] S W Stahler, F H Shu and R E Taam *Astrophys. J.* **241** 637 (1980)
- [45] S W Stahler *Publ. Astron. Soc. Pacific* **106** 337 (1994)
- [46] V M Goldschmidt *Skr. Nor. Vidensk. Acad. Oslo* **1** No 4 (1937)

- [47] H N Russell and W S Adams *Astrophys. J.* **68** 9 (1928)
- [48] A Unsold *Les Elements et Leurs Isotopes dans l'univers* (Liege : Univ. of Liege) p 7 (1979)
- [49] R K Parui *PhD Thesis* (Manipur Univ., Imphal, India) (1991)
- [50] R Arsenault, J-R Roy and J Boulesteix *Astron. Astrophys.* **234** 23 (1990)
- [51] R Canal, E Carcia-Berro, J Isern and J Labay in *Proc. 7th Workshop on Nuclear Astrophysics MPA/P7* (Max Planck Institute, Garching, Germany) p 7 (1993)
- [52] P Qiu-he in *4th MPG-CAS Workshop on High Energy Astrophysics and Cosmology MPA/P8* (Max Planck Institute, Garching, Germany) p 74 (1993)
- [53] C J Lada in *Proc. XXVII ESLAB Symposium on Frontiers of Space and Ground Based Astronomy* eds. W Wamsteckar, M Longair and Y Kondo (Netherlands : Kluwer Academic) in Press (1994)
- [54] R P Kraft *Publ Astron. Soc. Japan* **106** 553 (1994)
- [55] V Korchagin, A Kembhavi, Y D Mayya and T P Prabhu *Inter. Univ. Centre for Astron. Astrophys. India Preprint No : IUCAA-17/94* (1994)
- [56] M Beech and R Mitalas *Astrophys J Suppl* **95** 517 (1994)
- [57] H Reeves *Stellar Evolution and Nucleosynthesis* (NY : Gordon & Breach) p 75 (1968)
- [58] E E Salpeter *Astrophys J* **115** 326 (1952)
- [59] E E Salpeter *Ann Rev Nucl Sci* **2** 41 (1953)
- [60] E J Opik *Proc Royal Irish Acad.* **A54** 49 (1951)
- [61] E J Opik *Memo Socy Roy Sci Liege* **14** 131 (1954)
- [62] F Hoyle and M Schwarzschild *Astrophys J Suppl.* **2** 1 (1955)
- [63] C A Barnes in *Essays in Nucl. Astrophys.* eds C A Barnes, D D Clayton and D N Schramm (Cambridge : Cambridge Univ Press) p 199 (1982)
- [64] F Hoyle, D N F Dunbar, W A Wenzel and W Whaling *Phys Rev.* **92** 1095 (1953)
- [65] C W Cook, W A Fowler, C C Lauritsen and T Lauritsen *Phys Rev* **107** 508 (1957)
- [66] C A Barnes in *Ref* **63** p 193 (1982)
- [67] D E Alburger *Phys Rev* **124** 193 (1961)
- [68] P A Seeger and R W Kavanagh *Astrophys J* **137** 704 (1963)
- [69] I Hall and N W Tanner *Nucl Phys* **53** 673 (1964)
- [70] H Crannell, T A Griffy, L R Suelzle and M R Yearian *Nucl. Phys.* **A90** 152 (1967)
- [71] P Strehl and T H Schucan *Phys. Lett.* **B27** 641 (1968)
- [72] P Strehl and T H Schucan *Z. Phys* **234** 416 (1968)
- [73] A W Obst, T B Grandy and J Weil *Phys. Rev.* **C5** 1773 (1972)
- [74] D Chamberlin, D Bodansky, W W Jacobs and D L Oberg *Phys Rev.* **C9** 69 (1974)
- [75] C N Davids, R C Pardo and A W Obst *Phys Rev.* **C11** 2063 (1975)
- [76] H B Mak, H C Evans, C T Ewan, A B McDonald and T K Alexander *Phys. Rev.* **C12** 1158 (1975)
- [77] R G Karkham, S M Austin and M A M Shahabuddin *Nucl Phys* **A270** 489 (1976)
- [78] D E Alburger *Phys Rev.* **C16** 2394 (1977)
- [79] R G H Robertson, R A Warner and S M Austin *Phys. Rev.* **C15** 1072 (1977)
- [80] S M Austin, G F Treutleman and E Kashy *Astrophys. J. Lett.* **163** L79 (1971)
- [81] H Stocker, A A Rollefson and C P Browne *Phys Rev* **C4** 1028 (1971)
- [82] S J McCaslin, F M Mann and R W Kavanagh *Phys. Rev.* **C7** 489 (1973)
- [83] P L Jolivet, J D Goss, A A Rollefson and C P Browne *Phys. Rev.* **C10** 2629 (1974)

- [84] J A Nolen (Jr.) and S M Austin *Phys. Rev.* **C13** 1773 (1976)
- [85] C A Barnes and D B Nichols *Nucl. Phys.* **A217** 125 (1973)
- [86] P Dyer and C A Barnes *Nucl. Phys.* **A233** 495 (1974)
- [87] D C Weisser, J F Morgan and D R Thompson *Nucl. Phys.* **A235** 460 (1974)
- [88] J Humblet, P Dyer and B A Zimmerman *Nucl. Phys.* **A271** 210 (1976)
- [89] S E Koonin, T A Tombrello and G Fox *Nucl. Phys.* **A220** 221 (1974)
- [90] F C Barker in *Ref.* **28** p 163 (1990)
- [91] S E Woosley in *Proc. Accel. Radioactive Beams Workshop* eds L Buchmann and J M D' Auria TRIUMF Rep No : **TRI-85-1** p 275 (1985)
- [92] G R Caughlan and W A Fowler *Atomic Data Nucl. Data Tables* **40** 283 (CF88) (1988)
- [93] R Plaga *et al Nucl. Phys.* **A465** 291 (1987)
- [94] A Redder *et al Nucl. Phys.* **A462** 385 (1987)
- [95] R M Kremer *et al Phys. Rev. Lett.* **60** 1475 (1988)
- [96] F C Barker and P B Treacy *Nucl. Phys.* **38** 33 (1962)
- [97] C A Von Weizsacker *Z. Phys.* **39** 633 (1938)
- [98] J Audouze and V Vonclair *An Introduction to Nuclear Astrophysics* (Holland : D Riedel) Ch-Nucleosynthesis (1980)
- [99] H A Bethe in *Ref.* **63** p 439 (1982)
- [100] J L Greenstein *Modern Physics for Engineers* (NY : McGraw Hill) p 267 (1954)
- [101] A G W Cameron *Phys. Rev.* **93** 932 (1954)
- [102] W A Fowler, G R Burbidge and E M Burbidge *Astrophys. J.* **122** 271 (1955)
- [103] K R Lang *Astrophys. Formulae* (Hidelberg, Springer-Verlag) (1980)
- [104] J Audouze and V Vonclair *An Introduction to Nuclear Astrophys* (Holland : D Riedel) (1980)
- [105] A G W Cameron *Astrophys. J.* **121** 144 (1955)
- [106] M Schwarzschild and R Harm *Astrophys. J.* **150** 961 (1967)
- [107] R H Sanders *Astrophys. J.* **150** 971 (1967)
- [108] C N Davids *Nucl. Phys.* **A110** 619 (1969)
- [109] J K Bair and F X Haas *Phys. Rev.* **C7** 1356 (1973)
- [110] F Ramstrom and T Wiedling *Astrophys. J.* **211** 223 (1977)
- [111] A G W Cameron *Astrophys. J.* **65** 485 (1960)
- [112] C Charbonnel *Astron. Astrophys.* **282** 811 (1994)
- [113] G Schaller, D Schaerer, G Meynet and A Maeder *Astron. Astrophys. Suppl.* **96** 269 (1992)
- [114] D Schaerer, G Meynet, A Maeder and G Schaller *Astron. Astrophys. Suppl.* **98** 523 (1993)
- [115] D Schaerer, C Charbonnel, C Meynet, A Maeder and G Schaller *Astron. Astrophys. Suppl.* **102** 339 (1993)
- [116] C Charbonnel, G Meynet, A Maeder, G Schaller and D Schaerer *Astron. Astrophys. Suppl.* (in Press) (1993)
- [117] F J Rogers and C A Iglesias *Astrophys. J. Suppl.* **79** 507 (1992)
- [118] C A Iglesias, F J Rogers and B G Wilson *Astrophys. J.* **397** 717 (1992)
- [119] I Iben (Jr.) *Astrophys. J.* **147** 624 (1967)
- [120] D S P Dearborn, P P Eggleton and D N Schramm *Astrophys. J.* **203** 455 (1976)
- [121] C Sneden in *Evolution of Stars : The Photospheric Abundance Convection*, IAU Symp. **145** eds G Michaud and A Tutukov (Dordrecht : Kluwer Academic) p 235 (1991)

- [122] T T Greene *Astrophys. J.* **157** 737 (1969)
- [123] J A Brown *Astrophys. J.* **317** 701 (1987)
- [124] K K Gilroy and J A Brown *Astrophys. J.* **371** 578 (1991)
- [125] K K Gilroy *Astrophys. J.* **347** 835 (1989)
- [126] J A Brown and G Wallerstein *Astron. J.* **98** 1643 (1989)
- [127] V V Smith and N B Suntzeff *Astron. J.* **97** 6 (1989)
- [128] R A Bell, M M Briley and G H Smith *Astron. J.* **100** 187 (1990)
- [129] O Bienayme, A Maeder and E Schatzman *Astron. Astrophys.* **131** 316 (1984)
- [130] A V Sweigart and J G Mengel *Astrophys. J.* **229** 624 (1979)
- [131] M Arnould, G Paulus and A Jorissen *Astron. Astrophys.* **254** L9 (1992)
- [132] A Jorissen and M Arnould *Astron. Astrophys.* **221** 161 (1989)
- [133] P Decroock, Th Delbar, P Duhamel, W Gelster, M Huyse, P Leleux, I Licot, E Lienard, P Lipnik, M Loiselet, C Michotte, G Rychewaert, P Van Duppen, J Vanhorenbeeck and J Vervier *Phys. Rev. Lett.* **67** 808 (1991)
- [134] P Descouvemont and D Baye *Nucl. Phys.* **A500** 155 (1989)
- [135] F Ajzenberg-Selove *Nucl. Phys.* **A449** 53 (1986)
- [136] C E Rolfs and W S Rodney *Cauldrons in the Cosmos* (Chicago Chicago Univ. Press) (1988)
- [137] T E Chupp, R T Kouzes, A B McDonald, P D Parker, T F Wang and A J Howard *Phys. Rev. C* **31** 1023 (1985)
- [138] W A Fowler, G R Burbidge and E M Burbidge *Astrophys. J.* **122** 271 (1955)
- [139] R K Ulrich *Geochim. Cosmochem.* **46** 549 (1982)
- [140] I Iben *Astrophys. J.* **196** 525, 549 (1975)
- [141] K Wolke, C Rolfs, H P Trautvetter, V Harms, M Wiescher, K-L Kratz and J W Hammer in *Proc 5th Workshop on Nuclear Astrophysics MPA/P1* (Max Planck Institut, Garching) p 1 (1989)
- [142] G R Caughlan, W A Fowler, M J Harris and B A Zimmerman *Atomic Data Nucl. Data Tables* **32** 197 (CFHZ) (1985)
- [143] P Descouvemont *Phys. Rev. C* **36** 2206 (1987)
- [144] B L Berman, R L Van Hermet and C D Bowman *Phys. Rev. Lett.* **23** 386 (1969)
- [145] K Wolke, V Harms, H W Becker, J W Hammer, K-L Kratz, C Rolfs, U Schroder, H P Trautvetter, M Wiescher and A Wöhr *Z. Phys.* **A334** 491 (1989)
- [146] H W Drotleff, A Denker, J W Hammer, H Kneec, S Kuchler, C Rolfs, D Streit and H P Trautvetter in *Proc. Int. Symp. on Nucl. Astrophys. MPA/P4* (Max Planck Inst. Garching, Germany) p 181 (1990)
- [147] H W Drotleff, A Denker, J W Hammer, H Kneec, S Kuchler, C Rolfs, D Streit and H P Trautvetter in *Proc. 6th Workshop on Nuclear Astrophys. MPA/P5* (Max Planck Institut, Garching, Germany) p 23 (1991)
- [148] T R Wang, R B Vogelaar and Kavang *Phys. Rev. C* **43** (Preprint) (1991)
- [149] C M Raiteri, M Busso, R Gallino and G Picchio in *Ref 146* p 281 (1991)
- [150] N Prantzos, M Arnould and J P Arcoragi *Astrophys. J.* **315** 209 (1987)
- [151] M Busso, G Picchio, R Gallino and A Chieffi *Astrophys. J.* **326** 196 (1988)
- [152] H Beer, G Rupp, F Voss and F Kappeler in *Proc. Int. Workshop on Nucl. Astrophys MPA/P1* (Max Planck Institute, Garching, Germany) p 6 (1989)
- [153] T R Wang, R B Vogelaar and Kavang in *ref. 148* p 3 (1991)
- [154] R K Parui *Indian J. Phys.* **67B** 120 (1993)

- [155] W D Arnett and F-K Thielemann *Astrophys. J.* **295** 589 (1985)
- [156] J P Arcoragi, N Langer and M Arnould *Max Planck Institut Preprint No : MPA 559* (1990)
- [157] H Beer and F Voss *Preprint* (1991)
- [158] G Meynet and M Arnould *Int. Symp. on Nucl. Astrophys. 'Nuclei in Cosmos'* eds F Käppeler *et al* (UK : Inst. of Phys.) p 487 (1993)
- [159] H W Drotleff, A Denker, H Knee, M Soine, G Wolf, J W Hammer, U Greife, C Rolfs and H P Trautvetter *in Ref 158* p 197 (1993)
- [160] M Wiescher, F Kappeler, U Giesen, J Gorres, I Baraffe, M El Eid, C M Raiteri, M Busso and R Gallino *Preprint* (1994)
- [161] H W Drotleff, A Denker, H Knee, M Soine, G Wolf, J W Hammer, U Greife, C Rolfs and H P Trautvetter *Astrophys J* **414** 735 (1993)
- [162] M Wiescher, U Giesen, J Gorres, R E Azuma, K-L Kratz and H P Trautvetter *in Ref 158* p 191 (1993)
- [163] A Denker, H W Drotleff, M Grope, J W Hammer, H Knee, R Kunz, A Mayer, R S Seidel and G Wolf *in Ref 158* p 123 (1993)
- [164] P M Endt *Nucl. Phys.* **A521** 36 (1990)
- [165] A M Khokhlov *Astrophys. J.* **419** 200 (1993)
- [166] R G Gratton and C Sneden *Astron. Astrophys.* **287** 927 (1994)
- [167] M Sahrhling *Astron. Astrophys.* **284** 484 (1994)
- [168] N Itoh, T Adachi, M Nakagawa and Y Kohyama *Astrophys J.* **339** 354 (1989)
- [169] N Itoh, H Mutoh, A Hikita and Y Kohyama *Astrophys J.* **395** 622 (1992)
- [170] S Ichimaru and S Ogata *Astrophys. J.* **374** 647 (1991)
- [171] Y Rosenfeld *Phys. Rev.* **A46** 1059 (1992)
- [172] F-K Thielemann and W D Arnett *Astrophys. J.* **295** 604 (1985)
- [173] M Hashimoto, K Nomoto, T Tsujimoto and F K Thielemann *in Ref. 158* p 587 (1993)
- [174] R Gallino, C M Raiteri, M Busso and P Muttii *in Ref 158* p 90 (1993)
- [175] D Arnett *Astrophys J* **427** 932 (1994)
- [176] D K Nadyozhin *Astrophys J. Suppl.* **92** 527 (1994)
- [177] Zs. Nemeth, F Kappeler, C Theis, T Belgia and S W Yates *Astrophys J* **426** 357 (1994)
- [178] M D Leising *Astrophys J. Suppl.* **92** 495 (1994)
- [179] M J Kucher, R P Krshner, P A Pinto and B Leibundgut *Astrophys. J.* **426** L89 (1994)
- [180] M D Leising and G H Share *Astrophys. J.* **424** 200 (1994)
- [181] C M Raiteri, R Gallino, M Busso, D' Neuberger and F Kappeler *Astrophys J* **419** 207 (1993)
- [182] J M Deharveng, T P Sasseen, V Buat, S Bowyer, M Lampton and X Wu *Astron. Astrophys.* **289** 715 (1994)
- [183] R C Kennicutt and P C L Martin *in preparation* (1995)
- [184] R C Kennicutt *Steward Observatory Preprint* (1995)
- [185] L Blitz *in Giant Molecular Clouds in the Galaxy* eds. P Cassen and M G Edmunds (Oxford Pergamon Press) p 1 (1980)
- [186] V Buat, J M Deharveng and J Donas *Astron. Astrophys* **223** 42 (1989)
- [187] R C Kennicutt *Astrophys. J.* **344** 685 (1989)
- [188] V Buat *Astron. Astrophys.* **264** 444 (1992)
- [189] A Boselli *Astron. Astrophys.* **292** 1 (1994)

- [190] E J Shaya and S R Federman *Astrophys J.* **319** 76 (1987)
- [191] R P J Tilanus and R J Allen *Astrophys J. Lett* **339** L57 (1989)
- [192] R C Kennicutt, F Bresolin, D J Bomans, G D Bothum and I B Thompson *Astrophys J.* (in Press) (1995)
- [193] C L Taylor, E Brinks, R W Pogge and E D Skillman *Astrophys. J.* **107** 971 (1994)
- [194] J F Navarro and W Bens *Astrophys J.* **380** 320 (1991)
- [195] J F Navarro and S D M White *Mon. Not. Roy Astron. Soc.* **265** 271 (1994)
- [196] D Friedli and W Bens in *preparation* (1995)
- [197] L G Mundy, A Wootten, B A Wiling, G A Blake and A I Sargent *Astrophys J.* **385** 306 (1992)
- [198] C K Walker, J E Carlstrom and J H Beiging *Astrophys J.* **402** 655 (1993)
- [199] L G Mundy, B A Wilking and S T Myers *Astrophys J.* **311** L75 (1986)
- [200] M Montén, E Serabyn, R Gusten and T Wilson *Astron. Astrophys* **182** 127 (1987)
- [201] C K Walker, G Narayanan and A P Boss *Astrophys J.* **431** 767 (1994)
- [202] S Kwok *Publ. Astron. Soc. Pacific* **106** 344 (1994)
- [203] J Cowan, F-K Thielemann and J W Truran *Phys. Rep.* **208** 267 (1991)
- [204] G J Mathews, G Bazan and J J Cowan *Astrophys J.* **391** 719 (1992)
- [205] S E Woosley and E Baron *Astrophys. J.* **391** 228 (1992)
- [206] S E Woosley and R D Hoffman *Astrophys J.* **395** 202 (1992)
- [207] B S Meyer, W M Howard, G J Mathews, S E Woosley and R D Hoffman *Astrophys J.* **399** 656 (1992)
- [208] W M Howard, S Goriely, M Rayet and M Arnould *Astrophys. J.* **417** 713 (1993)
- [209] K Takahashi, H Th Janka and J Witt *Astron. Astrophys.* **286** 857 (1994)
- [210] K Takahashi, H Th Janka, J Witt and W Hillebrandt in *Proc. 6th Int. Conf. on Nuclei Far from Stability* eds R Neugart and A Wöhr (Institute of Physics - UK) p 839 (1993)
- [211] F Hoyle and W A Fowler *Astrophys J.* **132** 565 (1960)
- [212] R W Mayle and J R Wilson *Astrophys. J.* **334** 909 (1988)
- [213] S E Woosley, J R Wilson, G J Mathews, R D Hoffman and B S Meyer *Astrophys J.* **433** 229 (1994)
- [214] D S Miller, J R Wilson and R W Mayle *Astrophys. J.* **415** 278 (1993)
- [215] L H Aller *Astrophys J.* **432** 427 (1994)
- [216] A Shankar and D Arnett *Astrophys J.* **433** 216 (1994)
- [217] P Corvisiero, M Anghinolfi, G Ricco, M Sanzone, M Rauti and A Zucchiatti *Nucl. Phys.* **A526** 141 (1991)
- [218] A Zucchiatti, R W Fearick, J P F Sellschop and D G Aschman *Nucl. Phys.* **A575** 317 (1994)
- [219] D S P Dearborn *Phys. Rep.* **210** 367 (1992)
- [220] G R Huss, I D Hutcheon, G J Wasserburg and J Stone *Lunar Planet. Sci.* **23** 563 (1992)
- [221] G R Huss, I D Hutcheon, A J Fahey and G J Wasserburg *Meteoritics* **28** 369 (1993)
- [222] G R Huss, A J Fahey, R Gallino and G J Wasserburg *Astrophys. J.* **430** L 81 (1994)
- [223] L R Nittler, R M Walker, E Zinner, P Hoppe and R S Lewis *Lunar Planet. Sci.* **24** 1087 (1993)
- [224] I D Hutcheon, G R Huss, A J Fahey and G J Wasserburg *Astrophys J.* **425** L 97 (1994)
- [225] M F El Eid in *Ref. 51* p 60 (1993)
- [226] M J Harris, D L Lambert and V V Smith *Astrophys. J.* **325** 768 (1988)
- [227] M F El Eid in *Ref. 225* p 63 (1993)
- [228] M J Harris and D L Lambert *Astrophys J.* **285** 674 (1984)
- [229] P G Wannier *Ann. Rev. Astron. Astrophys.* **18** 399 (1980)

- [230] V Landre, N Prantzos, A Auger, G Bogaert, A Levebre and K P Thibaud *Astron. Astrophys* **240** 85 (1990)
- [231] A I Boothroyd, I-J Sackman and G J Wasserburg *Astrophys J.* **430** L 77 (1994)
- [232] H Beer, G Walter and F Kappeler *Astrophys J.* **389** 784 (1992)
- [233] T A Weaver and S E Woosley *Phys. Rep.* **227** 65 (1993)
- [234] C M Rauteri, R Gallino, M Busso, D Neuberger and F Käppeler *Astrophys. J.* **419** 207 (1993)
- [235] W D M Rae and P R Keeling *Nucl. Phys.* **A575** 175 (1994)
- [236] W D M Rae and P R Keeling *Nucl. Phys.* **A575** 207 (1994)
- [237] C M Rauteri, R Gallino, M Busso, D Neuberger and F Kappeler *in Ref.* 234 p 220 (1993)
- [238] J M L Ouellet *et al Phys. Rev. Lett.* **69** 1986 (1992)
- [239] L Buchmann *et al Phys. Rev. Lett.* **70** 726 (1993)
- [240] C Sneden, R P Kraft, C F Prosser, G E Langer and M D Shetrone *Astrophys J.* **107** 1773 (1994)
- [241] B J Armosky, C Sneden, G E Langer and R P Kraft *Astron. J.* **108** 1364 (1994)
- [242] A M Boesgaard and J R King *Astron. J.* **106** 2309 (1993)
- [243] J R King *Astron. J.* **106** 1206 (1993)
- [244] J R King *Astron. J. Preprint* (1994)
- [245] J R King *PhD Thesis* (Univ of Hawaii, USA) (1993)
- [246] J R King *Astrophys J.* **436** 331 (1994)
- [247] J R King and A M Boesgaard *Astron. J.* **109** 383 (1995)
- [248] R S Sutherland and M A Dopita *Astrophys. J.* **439** 365 (1995)
- [249] R S Sutherland and M A Dopita *Astrophys J.* **439** 381 (1995)
- [250] B Barbay and M Erdelyi-Mendes *Astron. Astrophys* **214** 239 (1989)
- [251] B Barbay in *Cool Stars, Stellar System and the Sun* ed. G Wallerstein (ASP, San Francisco) p 328 (1990)
- [252] M S Bessell, R S Sutherland and K Ruan *Astrophys J.* **383** L 71 (1993)
- [253] C Abia and R Rebolo *Astrophys J.* **347** 186 (1989)
- [254] R Altrock *Solar Phys.* **5** 260 (1968)
- [255] D L Lambert *Mon. Not. Roy. Astron. Soc.* **182** 249 (1978)
- [256] D Kiseiman *Astron. Astrophys* **245** L 9 (1991)
- [257] W J Spiesman and G Wallerstei *Astrophys. J.* **102** 1790 (1991)
- [258] M Spite and F Spite *Astron. Astrophys.* **252** 689 (1991)
- [259] E Biemont, A Hibbert, M Godefroid, N Vaecq and B C Fawcett *Astrophys J.* **375** 818 (1991)
- [260] Y Takeda *Publ. Astron. Soc. Japan* **46** 53 (1994)
- [261] G Bazan and D Arnett *Astrophys J. Lett.* **433** L 41 (1994)
- [262] G Sigl *Phys. Rev. D (FERMILAB PUB-4/369 A)* (1995)
- [263] P Salati *Astroparticle Phys.* **2** 269 (1994)
- [264] H-Th Janka in *Proc. Frontier Objects in Astrophysics and Particle Physics (S.I.F., Bologna)* eds. F Giovannelli and G Mannocchi p 345 (1993)
- [265] J Witt, H-Th Janka and K Takahashi *MPI Preprint No. : 760* (1993)
- [266] K Takahashi, J Witt and H-Th Janka *MPI Preprint No. : 761* (1993)
- [267] W Hillebrandt and K Takahashi *CERN Report 76-13* (1976)
- [268] W Keil and H-Th Janka *Max Planck Institute Preprint* 816 (1994)

- [269] J Meissner, H Schatz, J Görres, H Herndl and M Wiescher *Phys. Rev. C* **53** 459 (1996)
- [270] C Iliadis, L Buchmann, P M Endt, H Herndl and M Wiescher *Phys. Rev. C* **53** 475 (1996)
- [271] C Sneden, A McWilliam, G W Preston, J J Cowan, D L Burris and B J Armosky *Astrophys. J.* **467** 819 (1996)
- [272] J R King *Publ. Astron. Soc. Japan* **106** 423 (1994)
- [273] J-F Gonzales and M C Artu *Astron. Astrophys.* **289** 209 (1994)
- [274] D Eryurt, H Kirbiyik, N Kiziloglu, R Civelek and A Weiss *Astron. Astrophys.* **282** 485 (1994)
- [275] C Charbonnel *Astrophys. J.* **453** L 41 (1995)
- [276] M Busso, D L Lambert, L Beglio, R Gallino, C M Raiteri and V V Smith *Astrophys. J.* **446** 775 (1995)
- [277] M A Eswaran *Indian J. Phys.* **70A** 53 (1996)
- [278] C S Shastri and P Susan *Indian J. Phys.* **70A** 63 (1996)

About the Reviewer

R. K. Parui did his MSc in Physics in 1988 and PhD in 1993 from Manipur University. His field of specialization is Condensed Matter Physics. He is interested in the Astrophysical Condensed Matter Physics of Neutron Star and Pulsars, and has made original contribution in the behaviour of density variation parameter, internal magnetic field of neutron stars. At present, he is working on the behaviour of the Neutron star's internal magnetic field and Pulsar's radio emitting region magnetic field and its role towards understanding the physics of "Unified theory of Pulsar Radio Emission Mechanism" and Gravitational Wave source.